

Rejection of small charged and uncharged organic pollutants in reverse osmosis of salty and seawaters

Omar Samhari^{a,b}, Fatima Zohra Charik^{a,b}, Aissa Belouatek^{a,c}, Saad Alami Younssi^b, Murielle Rabiller-Baudry^{a,*}

^aUniversity Rennes, CNRS, ISCR (Institut des Sciences Chimiques de Rennes) – UMR 6226, F-35000, Rennes, France, emails: murielle.rabiller-baudry@univ-rennes1.fr (M. Rabiller-Baudry), omar.samhari@univ-rennes1.fr (O. Samhari), fatima.charik@univ-rennes1.fr (F.Z. Charik), abelouatek@gmail.com (A. Belouatek)

^bLaboratory of Materials, Membranes and Environment, Faculty of Sciences and Technologies of Mohammedia, University Hassan II of Casablanca, Morocco, email: saad.alamiyounssi@fstm.ac.ma (S.A. Younssi)

^cSEA2M Laboratory, Faculté des sciences exactes et de l'informatique, Université de Mostaganem, Algeria

Received 27 May 2021; Accepted 23 November 2021

ABSTRACT

Two organic solutes of close molecular weight ($\approx 270 \text{ g mol}^{-1}$) and hydrophobicity ($\log K_{ow} \approx 1.2\text{--}1.5$) were selected as model micropollutants to study their reverse osmosis in seawater. Tropaeolin O can be a monovalent/divalent anion whereas Thiamine can be a monovalent/divalent cation. Their charges and hydrophilic/hydrophobic balance can be modulated by playing on the pH and the ionic strength. The TFC-HR (Koch, USA) and SW30 (FilmTec, The Netherlands) membranes have shown a similar overall behavior either for single NaCl or Tropaeolin O filtrations. The comparison of Tropaeolin O/Thiamine rejections by the TFC-HR membrane has shown that membrane/solute electrostatic interactions explained the rejection in single solutions. However, in 30 g L^{-1} NaCl and synthetic seawater, rejections were more likely due to the hydrophobic/hydrophilic balance of a given solute: the more hydrophobic form being more rejected than the hydrophilic ones. Finally, the ethanol addition (30%) was achieved to study the impact of a second concentrated organics, moreover able to modify the background solvent of the filtration; Tropaeolin O rejection was decreased.

Keywords: Micropollutant; Transfer mechanism; Desalination; Reverse osmosis; Seawater; Azo dye; Vitamin; Tropaeolin O; Thiamine; Ethanol

1. Introduction

Today, at least one-third of the world's population lives in a country under water stress and the proportion could reach almost two-thirds by 2025 [1]. Reverse osmosis (RO) has progressively become the most widely used desalination process with respect to the less eco-efficient distillation [2–5]. Several countries, among which are North African ones [3], turned to the desalination of abundant seawater rather than brackish water even if the osmotic pressure limits the recovery of treated water to about 50% [6].

However, the salt's rejection that was the initial RO target is no longer sufficient and the treatment of the organic pollution of seawater due to industrial and human activities becomes an increasing issue [7,8] (especially in countries using seawater as a dustbin) inducing research challenges in membrane fabrication [9].

Besides the role of the osmotic pressure difference that controls the permeate flux, the solution–diffusion model is generally accepted to describe the solute transfer through the RO dense membranes [10]. Nevertheless, the leakage

* Corresponding author.

of small components in the permeate was reported, mainly for compounds with MW < 100 g mol⁻¹. For instance, the partial transmission of ethanol (46 g mol⁻¹) is well known for RO dealcoholization of wine, beer and distillery condensates [11–13]. Moreover, experimental proofs outlined the possible transmission of small organics of 200–300 g mol⁻¹ in the permeate side, regardless of the filtered fluid [14–22]. This raises a very interesting research question: how can small organic molecules pass through the RO polymer membranes, knowing that the size of certain ones (such as lactose MW = 342 g mol⁻¹, a neutral solute with a 0.42 nm radius [16]) could be close or greater than the estimated interstitial voids of a dense structure about 0.3 nm [23]? Although RO membranes were for a long time guessed as dense polymer, some of them were recently proved, from microscopic studies, to be heterogeneous and made of at least two phases instead of a single continuous dense one: (i) non-interconnected aqueous domains the continuity of which being did not still demonstrate and (ii) dense polymer domains [24–27] and perhaps an intermediate or interfacial phase making the link between the two previous ones [22]. This complex structure was suggested to be the origin of high-water flux because the dense polymer parts may account only for a fifth of the total water permeability [26]. Literature devoted to a nanofiltration (NF) widely reported on the conditions of rejection/transmission of neutral and charged solutes of about 300 g mol⁻¹ at a concentration in the mmol L⁻¹ range but currently few are known for RO of similar solutes and this gap has to be filled.

Inspired by NF and RO experimental results, it is becoming more and more clear that the physicochemical interactions between the polymer membrane and the organic solutes need to be considered with a more accurate approach, either for single solutes or those filtered in the mixture, moreover in complex media such as seawater. The use of a global partition coefficient (adsorption) at the membrane wall-based only on the intrinsic affinity between the polymer membrane and the solute appears progressively a too simple approach. It is also necessary to consider the physicochemical environment (pH, ionic strength, chemical nature of salts, other solutes able to adsorb on the membrane) that could modulate this affinity. In the same way, the modulation of the diffusion inside the heterogeneous structure of the membrane must be considered by integrating more accurately the changes of domains in the RO membrane (above) but also the physicochemical interactions which could be expressed with variable intensities in the membrane according to these domains. This will probably bring to fill the gap between NF and RO transfer mechanisms. As a general trend, two major phenomena have to be considered when dealing with the adsorption step at the membrane wall: the balance of the hydrophobic/hydrophilic interactions and that of the attractive/repulsive electrostatic interactions developed between the membrane and the solute.

On the one hand, hydrophobic interactions are known to increase with the ionic strength (*I*) increase; it is, for instance, the basis of hydrophobic interaction chromatography (HIC). In water applications, the “intrinsic” hydrophobicity of a solute is commonly appreciated at first sight

from its log K_{ow} where K_{ow} is the partition coefficient of the solute between water and octanol. Heo et al. [21] reported on the correlation of log K_{ow} to the binding energy between several organic solutes and a RO membrane (BW30) leading to favorable adsorption and higher rejection. However, exceptions were evidenced depending on the organic solute structure and its ability to π - π stacking and hydrogen bonding. On the second hand, electrostatic interactions between the charged polyamide membrane and a charged organic solute could be decisive: adsorption can be decreased in the case of repulsion or increased up to significant fouling in the case of attraction. Nevertheless, Heo et al. [21] reported on the negligible impact of the pH variation with respect to the adsorption for a set of ionizable compounds. These authors considered that log K_{ow} was a better descriptor than the pH. We draw from their conclusion that hydrophobic interactions were predominant toward electrostatic ones in the adsorption of the selected compounds.

To date, the use of log K_{ow} appears to be a step beyond the understanding of small organics’ transfer through RO membrane. However, for similar log K_{ow} is the transfer always the same through a given membrane? Aiming at answering this question to go ahead in better comprehension, two organic solutes (Tropaeolin O and Thiamine) of close molecular weight of about 270 g mol⁻¹ and close log K_{ow} (1.5–1.2) were selected as models in this systematic RO study. By varying the pH, Tropaeolin O can be a monovalent/divalent anion whereas Thiamine can be a monovalent/divalent cation. This means that, for each one of these solutes, the overall hydrophobicity was able to change: by increasing charges on a given chemical structure its hydrophilicity increases but the phenomenon can be screened by a significant ionic strength of about 0.5–0.6 mol L⁻¹ (that of seawater). Moreover, simultaneously the electrostatic interactions can be developed due to charges existing both on the membrane and the solutes. Knowing (i) that electrostatic interactions decrease with increasing ionic strength and (ii) that the intensity of hydrophobic interactions varies in the opposite direction, how will the balance of these two forces be managed at different pHs and in different saline environments?

Aiming at providing an answer, the 2 selected model molecules were filtered at acid and slightly alkaline pHs (4.5–4.9 and 7.5–8.2) either in a single solution or in NaCl and synthetic seawater. Two RO membranes (TFC-HR, Koch, USA and SW30, FilmTec, The Netherlands) were used. Results will also be discussed by considering the Hansen–Hildebrand solubility parameters of the solutes and the membranes as it is the common approach in organic solvent nanofiltration to discuss solute/membrane affinity.

2. Materials and methods

2.1. Water and solutes

2.1.1. Water

Tap water was deionized up to a resistance of 18 M Ω and 1 μ m filtered prior use. This deionized (DI) water was then used for the preparation of solutions that were further filtered in RO (water flux measurement, rinsing and cleaning).

2.1.2. Salt and synthetic seawater

Seawater composition is rather complex as more than 80 elements of the periodic table can be identified in its composition besides dissolved organic matter [28] (Table 1). Moreover, the salt composition is different with respect to the origin (Atlantic Ocean, Pacific Ocean, Mediterranean Sea, etc.).

For the sake of reproducibility, we have prepared synthetic seawater with a composition as close as possible to that of the Atlantic Ocean. The synthetic seawater was obtained by dissolving a commercially formulated mixture of sea salts (Instant Ocean) provided by Aquarium Systems (France) that must be used at 36 g L⁻¹ (density = 1.023) in marine aquaria.

This synthetic seawater (Table 1) contains cations among which the major ones (in the mmol L⁻¹ range) are: Na⁺, K⁺, Mg²⁺, Ca²⁺ and Sr²⁺ and anions that are mainly: Cl⁻, SO₄²⁻ as well as several species deriving from boron and carbon dioxide. Boron chemistry is quite complex and several anionic forms co-exist among which is the monovalent metaborate B(OH)₄⁻ and the divalent tetraborate B₄O₇²⁻, this last one favoring the precipitation of a sodium salt known as borax. All these forms are commonly referred as total boron (TB). The dissolution of CO₂ in water leads also to a complex system in which monovalent hydrogenocarbonate HCO₃⁻ and divalent carbonate CO₃²⁻ balance; there overall mixture is referred as the total carbon dioxide (TCO₂). The ionic balance is reached within less than 4% error when only considering these main ions. Besides these main components are those in the μmol L⁻¹ range. A detailed composition of “Instant Ocean” sea salt was reported by the study of Atkinson and Bingman [29].

The pH of this synthetic seawater was regularly measured at 8.2 ± 0.2 and the conductivity at 44.1 ± 0.6 mS cm⁻¹ (25°C).

The ionic strength ($I = 0.65 \text{ mol L}^{-1}$) was estimated by Eq. (1) from the main ions of Table 1.

$$I = \sum_i C_i z_i^2 \quad (1)$$

where C_i is the molar concentration of solute i (mol L⁻¹); z_i is the net charge of the ion i .

The osmotic pressure was estimated from the composition of Table 1 using the van't Hoff equation [Eq. (2), Table 2], highlighting a negligible variation between 25°C and 30°C (temperature range during RO filtration).

$$\pi = \sum_i RTC_i \quad (2)$$

where π is the osmotic pressure (atm), assuming 1 bar = 1 atm; C_i is the molar concentration of solute i (mol L⁻¹); R is the ideal gas constant (0.08205 L atm mol⁻¹ K⁻¹); T is the temperature (K).

For the sake of comparison, NaCl solutions were prepared at concentrations ranging from 15 to 45 g L⁻¹. Sodium chloride (NaCl, 58.44 g mol⁻¹) of analytical grade (99.74%) was purchased from Fisher Scientific (Waltham, Massachusetts, USA). The theoretical osmotic pressures were calculated using the van't Hoff equation [Eq. (2), Table 2]. Based on these estimations, 30 g L⁻¹ NaCl could be a relevant concentration for further comparison to the synthetic seawater filtrations. However, increasing concentrations could

Table 1

Main ions of the “Instant Ocean” salt mixture used for the synthetic seawater preparation ($d = 1.023$) and calculated osmotic pressure for each element according to Eq. (2)

Ions	Seawater [28]		Synthetic seawater [29]				Osmotic pressure (bar)	
	MW (g mol ⁻¹)	mmol kg ⁻¹	mmol kg ⁻¹	mmol L ⁻¹	g L ⁻¹	at 25°C	at 30°C	meq L ⁻¹
Main cations								581
Na ⁺	22.99	470	462	452	10.38	11.042	11.228	452
K ⁺	39.10	10.2	9.4	9.2	0.36	0.225	0.228	9.2
Mg ²⁺	24.31	53	52	51	1.24	1.243	1.264	102
Ca ²⁺	40.08	10.3	9.4	9.2	0.37	0.225	0.228	18.4
Sr ²⁺	87.62	0.09	0.19	0.19	0.02	0.005	0.005	0.37
Main anions								557
Cl ⁻	35.45	550	521	509	18.06	12.453	12.661	509
SO ₄ ²⁻	96.06	28	23	22.5	2.16	0.550	0.559	45
TCO ₂	61.02 ^a	1.90	1.90	1.90	0.11 ^a	0.046	0.047	1.90
TB	78.84 ^b	0.42	0.44	0.43	0.03 ^b	0.011	0.011	0.86
				Total		25.8	26.2	
							cations – anions	24
							(cations – anions)/cations	4%

^awhen considering only hydrogenocarbonate form;

^bwhen considering only borate form.

Table 2

Theoretical osmotic pressure (bar) of the synthetic seawater (Table 1 for composition) and NaCl solutions calculated according to the van't Hoff equation [Eq. (2)]

Concentration (g L ⁻¹)	Synthetic seawater				NaCl			
	36	15	25	30	35	40	45	50
25°C	25.8	12.6	20.9	25.1	29.3	33.5	37.7	41.8
30°C	26.2	12.8	21.3	25.5	29.8	34.0	38.3	42.5

be used aiming at modeling a RO concentration step. With respect to the limitation of our pilot (46 bars), the maximum concentration of use was estimated at 50 g L⁻¹ considering a full rejection of NaCl (not fairly true). The pressure upper limit of the membrane has also to be considered (below).

2.1.3. Tropaeolin O

Tropaeolin O (Fig. 1, CAS number = 547-57-9, $\log K_{ow} = \log P = 1.53$ [30]), also known as Orange 6 Acid or Yellow Resorcinol, is a water-soluble organic azo dye. Its molecular weight is 293.3 g mol⁻¹ in acid form (C₁₂H₉O₅N₂S). It is commercialized as a monovalent sodium salt (C₁₂H₈O₅N₂S Na, 316.3 g mol⁻¹, Tropaeolin O, pure, Sigma-Aldrich, St. Louis, USA).

Tropaeolin O was used at a concentration of 0.5 mM for RO filtration. With respect to the pH, either 4.8 (single solution) or 7.5–7.8 (in NaCl, pH adjusted by NaOH addition) its average net charge was $z = -1.1$ or -1.7 , respectively; corresponding to mixtures of 94/6 and 0.6/99.4 mol/mol monovalent/divalent anions, respectively. In synthetic seawater, Tropaeolin O is a divalent anion.

2.1.4. Thiamine

Thiamine, also called Vitamin B1, is soluble in water ($\log K_{ow} = \log P = 1.19$ [31], Fig. 2, CAS number = 70-16-6). Its molecular weight is 265.3 g mol⁻¹. However, with respect to the pH, Thiamine can be alternatively a divalent or a monovalent cation, and can also exist in a zwitterionic neutral form at alkaline pHs greater than 9.2. Thiamine, commercialized in hydrochloride form (meaning divalent cation with 2 chloride counter anions, C₁₂H₁₇N₄OS Cl, HCl) was purchased from Acros Organics (Beel, Belgium).

Thiamine was used at a concentration of 0.5 mM for RO filtration. In solution, the natural pH at 0.5 mM was 4.5.

With respect to the pH, either 4.5 or 8.2 (NaCl with pH adjusted by NaOH addition) its average net charge is $+1.7$ or $+0.9$, respectively; corresponding to mixtures of 44/66 and 91/9 mol/mol monovalent/divalent cations, respectively. In synthetic seawater Thiamine average net charge is $z = +0.9$ (91/9 mol/mol monovalent/divalent).

2.1.5. Ethanol

Ethanol (46.1 g mol⁻¹, provided by VWR, France, 96.0 vol.%) was used as a small neutral solute aiming at modeling some organics, for instance, those spread in seawater during oil spills. The amount was voluntarily selected at a quite high level, namely 10% and 30% v/v in water

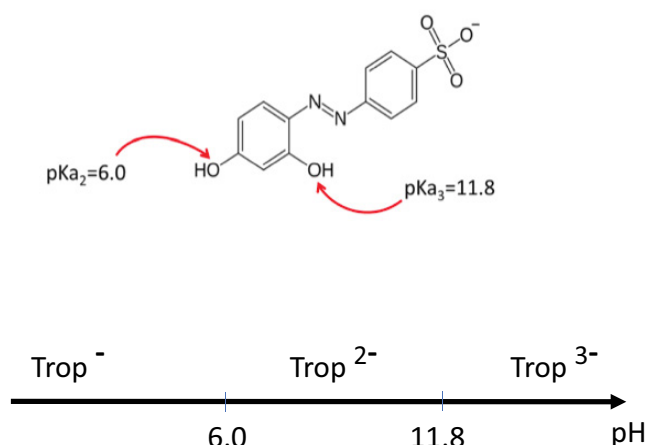


Fig. 1. Scheme and charges of Tropaeolin O vs. pH ($pK_{a1} < 2$ for the sulfonate group always negatively charged, $pK_{a2} = 6.0$; $pK_{a3} = 11.8$).

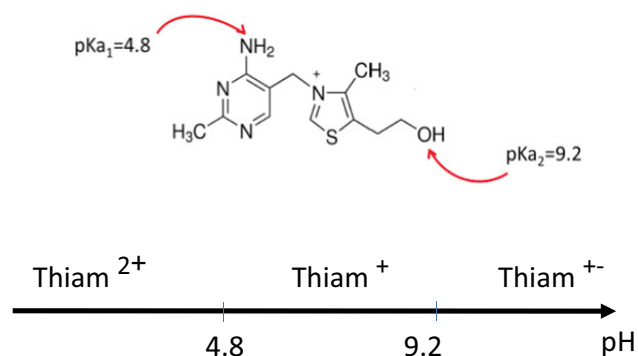


Fig. 2. Scheme and charges of Thiamine vs. pH (the quaternary ammonium N⁺ group is a strong base always positively charged, $pK_{a1} = 4.8$; $pK_{a2} = 9.2$).

corresponding to 1.7 and 5.1 mol L⁻¹, respectively. Moreover, as ethanol and water are fully miscible, ethanol is also allowed to model one possible impact of organics that are able to modify the solvent properties such as its density and its viscosity (Table 3).

2.1.6. Other reagents

NaOH pellets of analytical grade were purchased from Fisher Scientific (Waltham, Massachusetts, USA) and used to adjust the pH of Tropaeolin O and Thiamine solutions.

Table 3
Properties of water/ethanol mixtures at 20°C

Pure solvent or/mixtures v/v	Ethanol (mol L ⁻¹)	r_s (nm)	η (mPa·s)	ρ (g cm ⁻³)	π (bar)
Water		0.17	1.005	1.000	
Ethanol		0.31	1.189	0.791	
Water/ethanol 90/10	1.7		1.289	0.979	38
Water/ethanol 70/30	5.1		2.313	0.937	132

Stokes radius r_s , viscosity η , density ρ , osmotic pressure π , as reported by the study of Nguyen et al. [32].

Aiming at the removal of organics adsorbed on the RO membranes, cleaning in place was achieved at the transmembrane pressure of the “fouling” step for 30–60 min at room temperature using an alkaline formulated detergent (Ultrasil 10, 0.10–0.14 g L⁻¹, pH \approx 11, provided by Ecolab, Issy Les Moulineaux, France). It was checked that the cleaning effluents were colored after Tropaeolin O filtration proving its “irreversible adsorption” on the two selected membranes. It was also proved that two consecutive filtrations of Tropaeolin O with the SW30 membrane with a simple water rinsing (removing reversible fouling) or an alkaline cleaning (removing irreversible fouling) in between led to the same flux and rejection of the azo dye in both cases. These results suggested that adsorption was rapid when the membrane was in contact with the dye, regardless of the pH, and that a long adsorption time of a few hours is often suggested when filtering organics at a much lower concentration (in the $\mu\text{mol L}^{-1}$ range) was not necessary here.

2.2. Rejection and solute analysis

Rejection of a solute (R) was calculated according to:

$$R = 1 - \frac{C_p}{C_r} \quad (3)$$

where C_p is the concentration in the permeate; C_r is the concentration in the retentate.

2.2.1. Salts

The pH measurement of retentates and permeates (± 0.05) was carried out using a CRISON GLP 21 pH-meter equipped with temperature correction. It allowed to calculate the proton and/or OH⁻ rejection.

The conductivity ($\pm 0.1\%$) of NaCl solutions was measured with a CRISON GLP 31 conductivity meter equipped with a temperature correction at 25°C. The accuracy of NaCl rejection was estimated at 0.2%.

The conductivity of the retentates and permeates was also measured during synthetic seawater RO. As the conductivity is the combination of ion concentration and intrinsic ion conductivity, in absence of ion identification in the permeate, conductivity is only allowed to determine an apparent rejection of overall salts, without entering in ion transfer selectivity. Nevertheless, this apparent value was given as an indication because the present study mainly focused on the rejection of the organic components.

2.2.2. Tropaeolin O and Thiamine

Tropaeolin O and Thiamine were quantified from their UV absorbance (Abs) by the mean of the well-known Beer–Lambert Law:

$$\text{Abs} = \log\left(\frac{I_0}{I}\right) = \epsilon_\lambda \times \ell \times C \quad (4)$$

where ϵ_λ is the molar extinction coefficient at λ wavelength (L mol⁻¹ cm⁻¹); ℓ is the optical path length (1 cm); C is the concentration (mol L⁻¹).

UV spectra were acquired with a UV spectrometer (JASCO-V360, France). The maximum absorbance of Tropaeolin O was determined at $\lambda_{\text{max}} = 426 \pm 2$ nm over the studied pH range (Fig. 3a) whereas that of Thiamine was located at $\lambda_{\text{max}} = 238 \pm 3$ nm (Fig. 3b). The calibration was established for both solutes (Fig. 3c and d). Accordingly, the accuracy on rejection was estimated to be better than 0.2% for Thiamine and better than 0.3% for Tropaeolin O, respectively.

2.2.3. Ethanol

Ethanol in water was quantified by attenuated total reflection-Fourier-transform infrared spectroscopy (ATR-FTIR) by the mean of the Beer–Lambert Law [Eq. (4), in which $\epsilon_\lambda \times \ell$ is substituted by a coefficient accounting for the infrared beam pathway in the solution, the reflection of the ZnSe crystal of the ATR accessory and the intrinsic absorption of the sample at the selected wavenumber]. Spectra were acquired with a JASCO 4100 spectrometer (JASCO) equipped with an ATR-accessory owing a ZnSe crystal (mono-reflection, 45° infrared beam incidence angle). Each spectrum was obtained from 128 scans at 2 cm⁻¹ resolution, in the 3,700–600 cm⁻¹ wavelength range with a background registered in the air (Fig. 4a). The absorbance was measured at 1,045 cm⁻¹ (referred as H¹⁰⁴⁵) for which ethanol has a specific band assigned to the C–O vibration bond [33] and the water has no specific band. However, the absorbance of water at 1,045 cm⁻¹ was not null (non-specific absorbance) but equal to 0.0356 au (absorbance unit) when measured from a baseline selected in the 1,917–1,880 cm⁻¹ flat range of the spectrum. Calibration was obtained by plotting H¹⁰⁴⁵ vs. ethanol concentration (Fig. 4b). The accuracy of ethanol rejection was estimated at $\pm 10\%$.

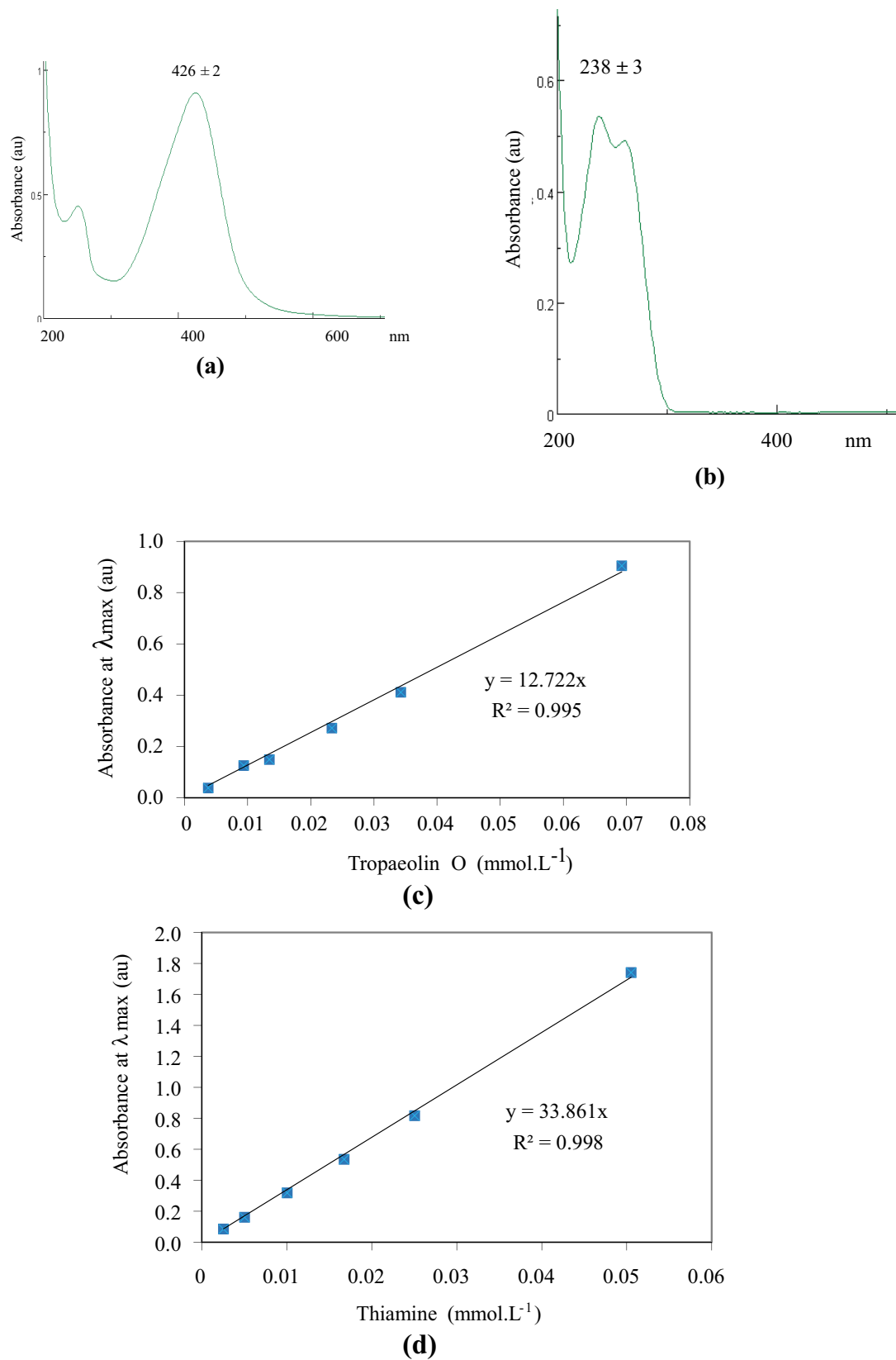


Fig. 3. UV spectra and calibration thanks to the Beer-Lambert Law for the two organic solutes: (a) UV spectrum of Tropaeolin O (≈0.1 mM, pH = 6.8) in water, (b) UV spectrum of Thiamine (≈0.04 mM, pH = 3.8), (c) Tropaeolin O calibration line in the 0.0037–0.0692 mmol L⁻¹ range and (d) Thiamine calibration line in the 0.0025–0.0505 mmol L⁻¹ range.

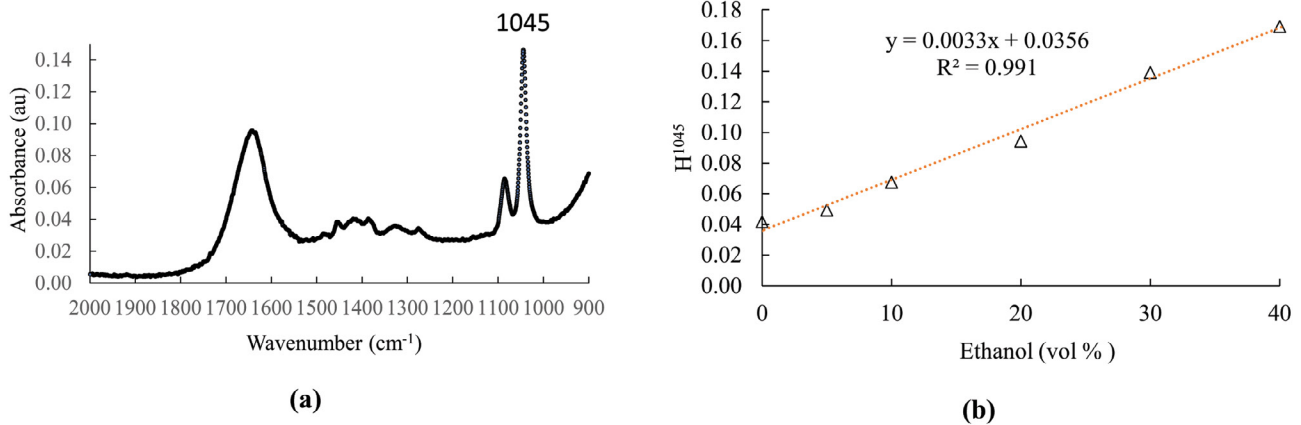


Fig. 4. ATR-FTIR of water/ethanol: (a) spectrum of water/ethanol 70/30 v/v, (b) calibration line according to the Beer–Lambert Law plotting the absorbance at 1,045 cm⁻¹ (ethanol specific band, baseline selected in the 1,917–1,880 cm⁻¹ to measure the absorbance) vs. the ethanol amount in water.

2.3. Membranes and filtration conditions

2.3.1. Membranes

Two different membranes were used. Both are polyamide thin film composite (TFC) membranes (Table 4). The first one, TFC-HR provided by Koch (USA), is a RO membrane widely used in food applications, the polyamide of which is a proprietary composition of Koch (USA) [34]. We have previously suggested that this membrane could be based on polypiperazine amide with respect to its ATR-FTIR spectrum [35]. The second one is a SW30 from Dow-FilmTec (The Netherlands) specially designed for seawater desalination and known to be an aromatic polyamide [36].

Whatever the membrane reference, flat membranes were sampled in their respective spiral membrane (2540 module type, ≈2.5 m² filtering area). Prior to filtration, the preservative was removed by soaking the membrane in deionized water.

The flat membrane of 140 cm² filtering area was then inserted in a plate and frame SEPA cell (GE Osmonics, USA). With respect to the two added shims, the free channel thickness was estimated at 1.25 mm. Moreover, a retentate spacer was inserted in the feed/retentate channel to increase turbulences and limit concentration polarisation and fouling (if any), as in a spiral membrane. Two types of spacers were used that have been collected in the spiral module corresponding to the membrane, namely a 31 mil diamond spacer for the TFC-HR membrane and an unspecified diamond spacer for the SW30 one.

2.3.2. RO experimental set-up and conditions

RO was achieved on a pilot designed for NF/RO by TIA (Bollène, France) equipped with the SEPA cell in which the flat RO was inserted (above).

The filtration was achieved by processing 10 L of solution at different transmembrane pressures (TMP) obtained by volunteer step-by-step increase of TMP in the studied range. With respect to the membrane stability toward TMP, it was from 15 to 36 bar with the TFC-HR and 15 to 46 bar for the SW30. The volume reduction ratio was $VRR = 1$ as

both the retentate and the permeate was fully recycled in the feed tank. In standard conditions, the temperature was 25°C (SW30) or 30°C (TFC-HR).

The feed flow rate was selected to be able to cover the overall studied TMP range. Thus, with respect to the pilot limits, the selection was different for each membrane. The feed flow rate was:

- $Q_{\text{feed}} = 210 \pm 10 \text{ L h}^{-1}$ corresponding to a cross-flow velocity close to 0.5 m s^{-1} (as estimated in the free channel) for the TFC-HR in water media.
- $Q_{\text{feed}} = 583 \pm 8 \text{ L h}^{-1}$ corresponding to a cross-flow velocity close to 0.8 m s^{-1} (as estimated in the free channel) for the TFC-HR in water/ethanol media.
- $Q_{\text{feed}} = 1,075 \pm 25 \text{ L h}^{-1}$ corresponding to a cross-flow velocity close to 2.5 m s^{-1} (as estimated in the free channel) for the SW30.

2.3.3. Calculations

Prior to use, a new RO membrane was first compacted in DI water during about 1 h at 46 bar, 25°C (SW30) or 36 bar, 30°C (TFC-HR), that was a sufficient time to reach a plateau value of flux (hereafter referred as J_0) and its corresponding permeance (hereafter referred as L_{p0}) with respect to the Darcy equation:

$$J_p = L_p \times \text{TMP} \quad (5)$$

where J_p is the permeate flux ($\text{L h}^{-1} \text{ m}^{-2}$); L_p is the membrane permeance ($\text{L h}^{-1} \text{ m}^{-2} \text{ bar}^{-1}$); TMP is the transmembrane pressure (bar).

The accuracy on J_p was estimated to be better than 3%. The precision on TMP was estimated close to 7% below 20 bar and close to 10% in the 25–46 bar range.

After any RO of salty mixtures (with or without any additional organics dissolved in, below), the membrane was carefully rinsed in filtration condition with DI water. The following water flux measured in DI water is hereafter referred as J_{rinsed} . When $J_{\text{rinsed}} = J_0$, it means that no irreversible

Table 4
Characteristics of the RO membranes according to their respective provider [34,36]

Membrane	Membrane material	Permeance (L h ⁻¹ m ² bar ⁻¹)	NaCl rejection		pH range stability	Maximum pressure (bar)
			Pressure (bar)	Rejection		
TFC-HR	Polyamide/Polysulfone	2.03	15.5	99.5 (2 g L ⁻¹)	4–11	41
SW30	Polyamide/Polysulfone	2.15	55	99.4 (32 g L ⁻¹)	2–11	69

fouling was evidenced on the membrane. Nevertheless, the existence of fouling due to organics (Thiamine or Tropaeolin O) can always be suspected, with respect to hydrophobic interactions that can be established between the polymer membrane and these solutes. However, this low fouling cannot be evidenced by DI water flux recovery. Consequently, a cleaning in place step was sometimes preventively achieved with an alkaline formulated detergent (Ultrasil 10, above). Finally, after a careful final DI water rinsing, the following water flux measured in DI water was determined and is hereafter referred as J_{cleaned} . When $J_{\text{cleaned}} = J_{\text{rinsed}}$ (general case) its value is not given in the following for the sake of simplification.

During RO of NaCl, leading to a difference in osmotic pressure between the retentate and permeate sides ($\Delta\pi$), the flux must be expressed according to:

$$J_p = L_p (\text{TMP} - \Delta\pi) \quad (6)$$

where

$$\Delta\pi = \pi_{\text{feed, membrane}} - \pi_{\text{permeate}} \quad (7)$$

where π_{permeate} is the permeate osmotic pressure; $\pi_{\text{feed, membrane}}$ is the osmotic pressure at the membrane wall, accounting for concentration polarisation.

The concentration polarisation modulus (M) can be simply estimated by [37,38]:

$$M = \frac{\pi_{\text{feed, membrane}} - \pi_{\text{permeate}}}{\pi_{\text{feed}} - \pi_{\text{permeate}}} = \frac{\text{TMP} \left[1 - \frac{J_{p(\text{salt})}}{J_{p(\text{DI water})}} \right]}{\pi_{\text{feed}} - \pi_{\text{permeate}}} \quad (8)$$

where π_{feed} is the osmotic pressure of the bulk feed; $J_{p(\text{DI water})}$ is the permeate flux in DI water; $J_{p(\text{salt})}$ is the permeate flux in salt solution; $M \gg 1$ means that significant concentration polarization occurs.

The J_p vs. TMP plot allows measuring $\Delta\pi_0$ by extrapolation at $J_p = 0$ (Fig. 5). $\Delta\pi_0$ maximum value is the osmotic pressure of the retentate (=feed) in absence of concentration polarization. When the rejection is constant over the feed pressure range and in absence of both concentration polarization (CP) and fouling, the slope of the straight-line remains equal to L_{p0} .

2.4. Streaming current measurement and zeta potential calculation

The membrane characterization was achieved according to a protocol already described by the study of Hanafi

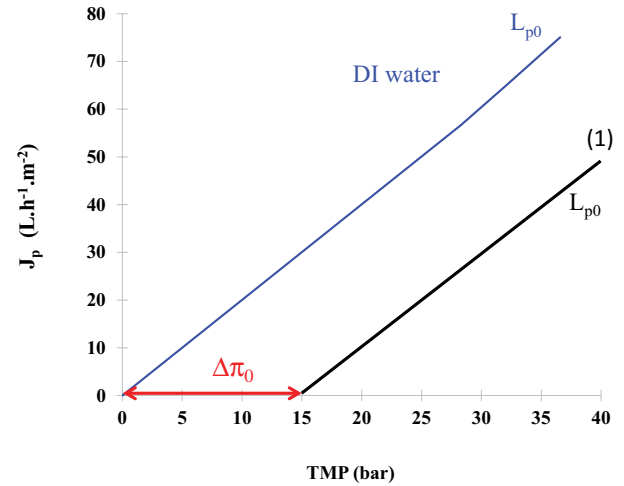


Fig. 5. Flux vs. TMP to show the experimental determination of $\Delta\pi_0$ when comparing DI water flux and water flux in NaCl for instance (1).

et al. [39]. A SurPASS Electrokinetic Analyzer (Anton Paar GmbH, Graz, Austria) equipped with an adjustable-gap cell was used to measure tangential streaming current. Membranes samples were cut and adjusted to the sample holder dimensions (2 cm × 1 cm) and fixed using double-sided adhesive tape. The distance between the membrane samples was set to $100 \pm 2 \mu\text{m}$. The solution flow was created by a pair of syringe pumps and streaming current was measured with a pair of reversible Ag/AgCl electrodes (surface area: 10 cm²). Using electrodes with a large surface area and alternating the direction of solution flow limits electrode polarization during streaming current measurements. The streaming current (I_s) was measured and recorded for increasing pressure differences up to 300 mbar, the flow direction being changed periodically. Prior to the first measurement the electrolyte solution was circulated through the channel formed by the membrane samples for at least 2 h in order to equilibrate the membrane samples with the background solution (1 mmol L⁻¹ KCl at the appropriate pH in water or water/ethanol mixture). All experiments were performed at room temperature ($20^\circ\text{C} \pm 2^\circ\text{C}$) under a controlled atmosphere (nitrogen gas) in order to allow accurate measurements at alkaline pHs. The zeta potential (ζ) was deduced from its relationship with the streaming current (I_s) according to:

$$I_s = \frac{Wh_{\text{ch}} \epsilon_0 \epsilon_r \Delta P^\circ}{\eta L} \zeta \quad (9)$$

Table 5

Hansen–Hildebrand solubility parameters (δ), molar volume (V_m) calculated according to the Fedor method and deduced radius assuming a spherical shape for all solutes

Compounds	δ (J cm ⁻³) ^{1/2}	V_m (cm ³ mol ⁻¹)	Radius (nm)	$ \delta_{\text{solute}} - \delta_{\text{PPyPA}} $	$ \delta_{\text{solute}} - \delta_{\text{PA}} $
Ethanol	25.7	59.6	0.42	0.1	-10.1
Tropaeolin O	31.7	149.4	0.57	6.1	-4.1
Thiamine	28.9	28.9	0.60	3.3	-6.9
Polypiperazine amide (PPyPA)	25.6				
Fully aromatic Polyamide (PA)	35.8				

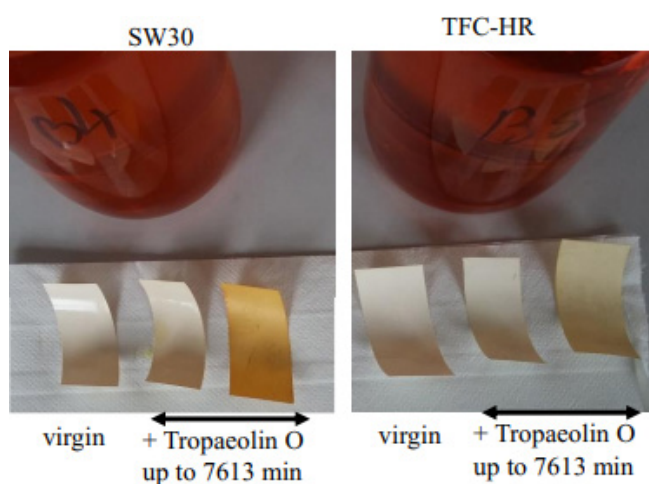


Fig. 6. Pictures of orange solution of dye and of membranes before and after adsorption of Tropaeolin O without draining and DI water rinsing to easily evidence the dye adsorption (either reversible and irreversible adsorption).

where h_{ch} is the channel thickness between the two membrane samples; ΔP° is the pressure difference along the channel formed by the two membrane samples; W and L are the width and length of the channel, respectively; η is the dynamic viscosity of the solution either that of water or of water/ethanol; ϵ_r is the dielectric constant of the solution either that of water or of water/ethanol; ϵ_0 is the permittivity in the void.

2.5. Hansen–Hildebrand solubility parameter and molar volume calculation

To tackle the impact of the affinity between a solute and a membrane and its impact on the rejection, the difference between their Hansen–Hildebrand solubility parameters and that of the membranes were calculated, knowing that the higher is the affinity the closer are their respective parameters.

Hansen–Hildebrand solubility parameter (δ) was determined by the group contribution method proposed by Fedors [40]. For this purpose, either the solute or the unit block of the polymer membrane was “cut” into its functional groups and structural fragments. Each group has cohesion energy ($E_{\text{coh},i}$) and a molar volume ($V_{m,i}$) which were found in a referent table provided in [40]. The

solubility parameter δ (J cm⁻³)^{1/2} was then calculated by the addition of the contribution of each fragment (Table 5).

Moreover, the molar volume of a solute can be deduced, allowing an estimation of its radius assuming a spherical shape (Table 5). Considering that ethanol radius is given at 0.3 nm in current literature, the comparison with the calculation evidence that the solute size was slightly overestimated by this method. Consequently, the size of Tropaeolin O and Thiamine was probably also slightly overestimated. Nevertheless, these calculations suggested that the two solutes have more or less the same size and that their solubility parameters were not significantly different. This last comment is in good agreement with the close values of their $\log K_{\text{ow}}$.

The solubility parameter difference (absolute value) evidenced that the affinity of Tropaeolin O is more or less the same for the two types of membranes whereas the affinity of Thiamine is slightly greater for the polypiperazine amide (PPyPA) than for the fully aromatic polyamide (PA) membrane (Table 5).

2.6. Irreversible adsorption of Tropaeolin O on the two membranes

The objective was to evaluate the irreversible adsorption of 0.5 mM Tropaeolin O on TFC-HR and SW30 membranes at room temperature in the 4.83–9.41 pH range used for RO experiments in order to evidence any difference in affinity between this solute in different physicochemical environments and both membranes. Adsorption experiments were achieved in solutions to which either 0 or 30 g L⁻¹ NaCl was added.

TFC-HR and SW30 membrane coupons (2 cm × 5 cm) were soaked up to 7,613 min in bottles containing 1 L Tropaeolin O solutions (-).

Following the adsorption and before ATR-FTIR analysis (below), the membrane coupons were rapidly drained and washed during 5 s with DI water in order to remove Tropaeolin O that was reversibly adsorbed. The membrane coupons were finally carefully dried in a desiccator under a dynamic vacuum for several days to remove water from membranes.

Adapting the quantification method of proteins on polymer membranes reported by Rabiller-Baudry et al. [41], ATR-FTIR analyses of dried membranes were performed to achieve a semi-quantification of the Tropaeolin O directly on the membranes. Spectra were recorded with JASCO 4100 spectrometer equipped with the same ATR crystal as

those described above for ethanol analysis (Section 2.2.3. – Ethanol).

Fig. 7 depicts typical ATR-FTIR spectra of the two membranes before and after Tropaeolin O adsorption (without rinsing to better evidence the selected bands). The spectrum of each one of the virgin membranes was the superimposition of the PA active layer spectrum and that of the intermediate layer made of polysulfone (PSU). The assignments of bands were already reported in [35] and to give more details here is out of the scope of this paper, except the band located at $1,238\text{ cm}^{-1}$ attributed to the C–O–C vibration band of PSU for the two membranes.

After Tropaeolin O adsorption a new band appeared on the two membranes, located at $1,033\text{ cm}^{-1}$ (Fig. 7) and logically attributed to the dye. It was checked that the PSU band at $1,238\text{ cm}^{-1}$ was without any superimposition with Tropaeolin O bands, allowing its use as an internal standard for quantification.

H^{1033} and H^{1238} were the absorbances at $1,033$ and $1,238\text{ cm}^{-1}$ measured thanks to the spectra manager software of the spectrometer, respectively (baseline $2,800\text{ cm}^{-1}$). An increase in H^{1033}/H^{1238} ratio means an increase in Tropaeolin O adsorption. However, the equations of the calibration curves relating the H^{1033}/H^{1238} absorbance ratio to the Tropaeolin O concentration on the membranes were not established because the preparation of controlled dye deposits on

membranes is very hard and long-time consuming work. Thus, only semi-quantification of Tropaeolin O on membranes was achieved, based on the variation (if any) of the H^{1033}/H^{1238} absorbance ratio.

3. Results

After determination of the zeta potential of both membranes and Tropaeolin O adsorption on the two membranes, RO of the synthetic seawater was first compared to that of NaCl at neutral pH and various concentrations aiming at identifying the NaCl concentration having the closer behavior (flux, salt rejection) to the synthetic seawater. Second, every organic solute was studied in a single solution, varying the pH from the natural acidic pH of the solution to the slightly alkaline one of the synthetic seawater. Then every organic compound was added either in NaCl solution or synthetic seawater to study the impact of the salts on the rejection of the charged organics. Finally, a ternary mixture made of Tropaeolin O, NaCl and ethanol was filtered aiming at the understanding impact of other organics at a very high concentration on the dye rejection.

3.1. Zeta potential of the TFC-HR and SW30 membranes

Fig. 8 depicts the zeta potential of both membranes in water. SW30 data were in good agreement with those

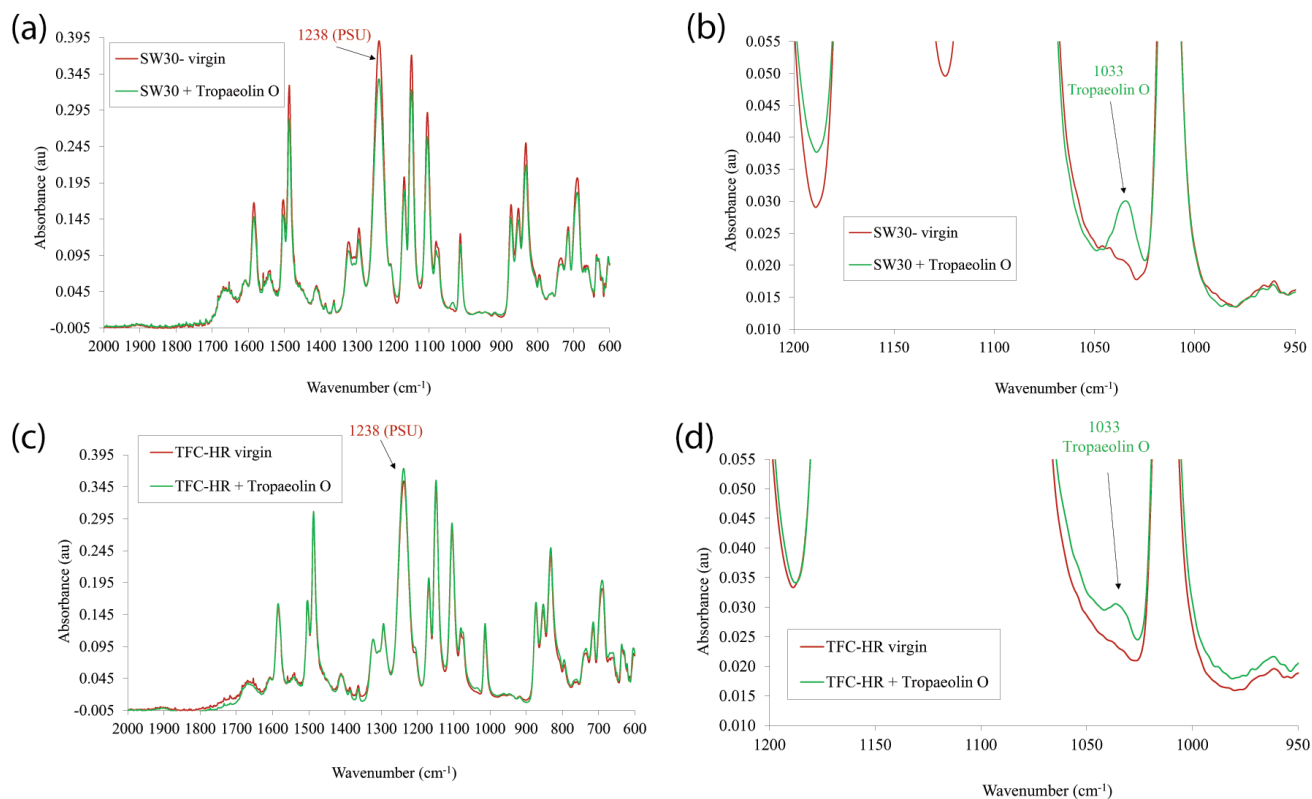


Fig. 7. ATR-FTIR spectra of the two virgin membranes highlighting the internal standard band of PSU at $1,238\text{ cm}^{-1}$ and spectra of the membranes after Tropaeolin O adsorption evidencing the $1,033\text{ cm}^{-1}$ band due to Tropaeolin O adsorption. (a) Spectra of SW30 virgin membrane and SW30 membrane after Tropaeolin O adsorption, (b) zoom of (a) in the $1,200\text{--}950\text{ cm}^{-1}$ region, (c) spectra of TFC-HR virgin membrane and TFC-HR membrane after Tropaeolin O adsorption and (d) zoom of (c) in the $1,200\text{--}950\text{ cm}^{-1}$ region.

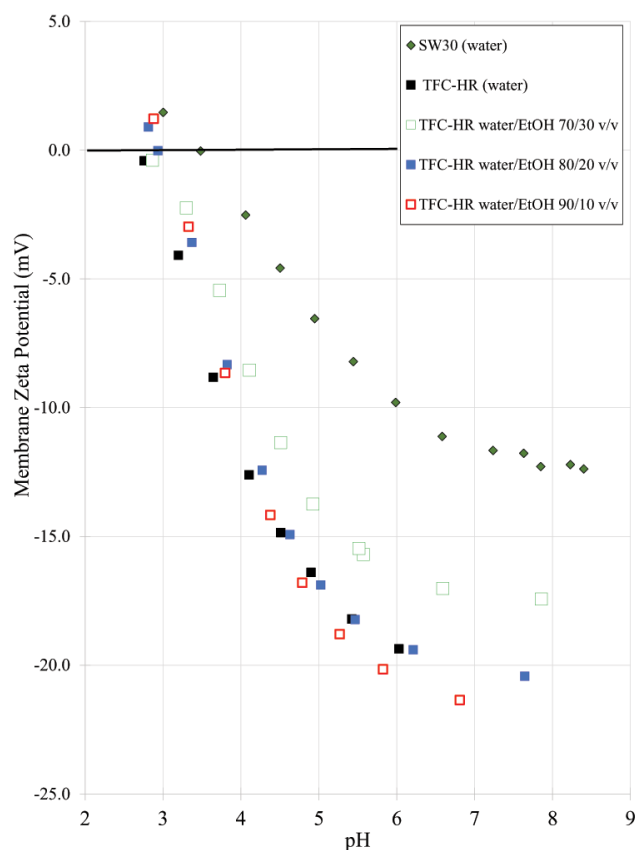


Fig. 8. Zeta potential of the TFC-HR and SW30 membranes was deduced from streaming current measurements in 1 mM KCl dissolved in various water/ethanol mixtures.

reported by the study of Li et al. [42] measured with the same equipment but using the streaming potential measurement instead of the streaming current as in the present study.

Besides a tight difference in their isoelectric point ($i_{ep} = 3$ for TFC-HR and $i_{ep} = 3.5$ for SW30), the comparison of the zeta potential of the two membranes suggests that the TFC-HR could be slightly more negative than the SW30 at the seawater pH = 8.2. This could have an impact on electrostatic interactions during RO if any ones take part in the transport/transfer mechanisms.

At first sight, the impact of ethanol dissolved in water up to 30 vol.% was not very significant on the TFC-HR membrane iep nor on its zeta potential at pH > iep.

3.2. Irreversible adsorption of Tropaeolin O on TFC-HR and SW30 membranes

Fig. 9 shows the membrane coupons after the irreversible adsorption of Tropaeolin O on the two membranes at various pHs and NaCl contents. The membranes were very slightly colored by the azo dye highlighting a low amount of Tropaeolin O irreversibly adsorbed on the two membranes regardless of the physicochemical environment.

Fig. 10 depicts the H^{1033}/H^{1238} ratio vs. the adsorption time. For a given membrane, roughly the irreversible Tropaeolin O adsorption was independent of the physicochemical

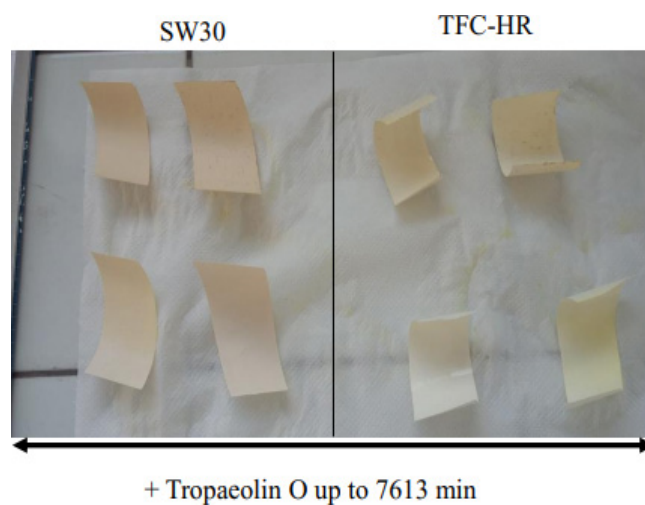


Fig. 9. Pictures of the two RO membranes after adsorption and slight water rinsing of Tropaeolin O at various pH and 0–30 g L⁻¹ NaCl highlight the low irreversible adsorption of the dye.

environment. These results suggest that the electrostatic repulsions account for a little and that hydrophobic interaction were likely those that were responsible for the dye adsorption. These results are in good agreement with those of Heo et al. [21] already mentioned in the introduction explaining that $\log K_{ow}$ is a better descriptor than the pH to deal with adsorption on RO membranes.

Moreover, the H^{1033}/H^{1238} ratios were roughly similar to the two membranes, suggesting closed Tropaeolin O adsorbed amounts on both membranes. This is in good agreement with the similar differences in the Hansen–Hildebrand parameters given in Table 5.

Finally, such results suggested that, for a given solute, if any rejection difference was observed when varying the physicochemical environment of the filtration, explanations of the different origins have probably to be found elsewhere than in membrane/solute affinity variations.

3.3. NaCl vs. synthetic seawater

The permeance of the two membranes in DI water was close $L_{p0} \approx 2.03\text{--}2.15$ L h⁻¹ m⁻² bar⁻¹ for TFC-HR and SW30, respectively.

3.3.1. Flux

Different concentrations of NaCl at neutral pH were filtrated ranging from 15 to 45 g L⁻¹ (Fig. 11). As expected, $\Delta\pi_0$ increases with NaCl concentration (Table 6). For a given TMP, the permeate flux decreased with the NaCl concentration increase. This is in good agreement with the increase of the osmotic pressure difference.

The osmotic pressure difference was calculated from the NaCl rejection (below) at every TMP for all NaCl concentrations, assuming no concentration polarisation ($\pi_{feed, membrane} = \pi_{feed}$, Table 2). The $\Delta\pi$ values matched well with the experimental $\Delta\pi_0$ (Table 6). The concentration polarisation modulus (M) was evidenced to be close to 1 (details

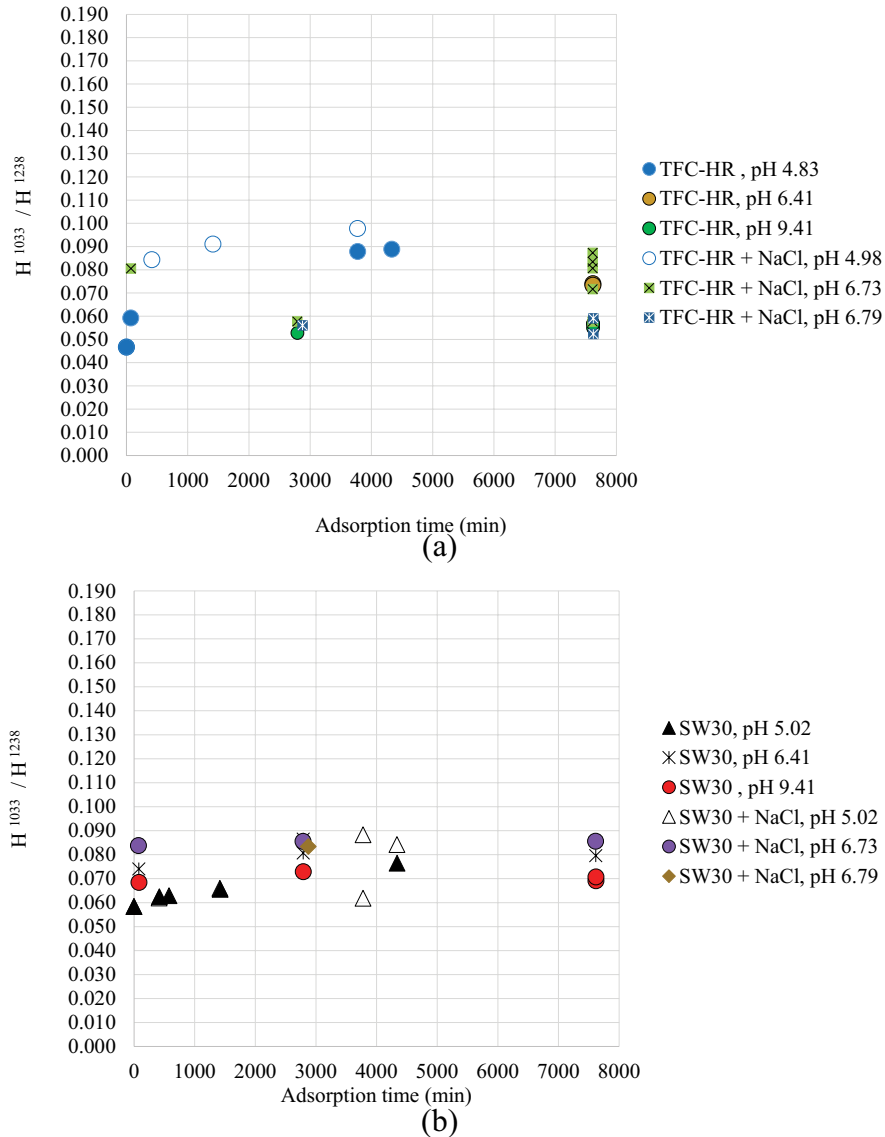


Fig. 10. Irreversible adsorption of 0.5 mM Tropaeolin O at different pHs in presence of 0 or 30 g L⁻¹ NaCl on (a) TFC-HR and (b) SW30 membranes at room temperature as drawn from ATR-FTIR measurement of the H^{1033}/H^{1238} absorbance ratio vs. immersion time up to 7,613 min.

not shown). Both results agreed with a negligible concentration polarisation.

The permeance in synthetic seawater is depicted in Fig. 11b and c highlighting their good accordance from one membrane to the other and with the 30 g L⁻¹ NaCl solution.

3.3.2. Rejections

The NaCl rejection by the two membranes was above 0.90 for $J_p \geq 5 \cdot 10^{-6}$ m s⁻¹ (Fig. 12a). The plateau value of rejection was close to 0.94–0.95 for both membranes in the 25–35 g L⁻¹ NaCl concentration range.

Fig. 12b compares the overall salts' rejections of seawater to the 30 g L⁻¹ NaCl ones. The agreement between the 2 sets of rejections was better with the TFC-HR membrane than with the SW30. However, no conclusion can be drawn as the

Table 6

$\Delta\pi_0$ measured with the TFC-HR membrane (\pm accuracy on TMP) and average $\Delta\pi$ calculated from feed osmotic pressure of Table 2 and rejection (\pm variation due to rejection)

NaCl (g L ⁻¹)	15	25	30	35
$\Delta\pi_0$ (bar)	12 \pm 1	17 \pm 3	21 \pm 3	25 \pm 4
$\Delta\pi$	12.4 \pm 0.1	20.0 \pm 0.2	23.6 \pm 0.6	27.7 \pm 0.4

conductivity measurement in seawater retentate/permeate was not able to reflect the only NaCl behavior.

Table 7 sums up the results with 30–35 g L⁻¹ NaCl and synthetic seawater. A result that raises the question is the evolution of the pH in the permeate. In NaCl solutions,

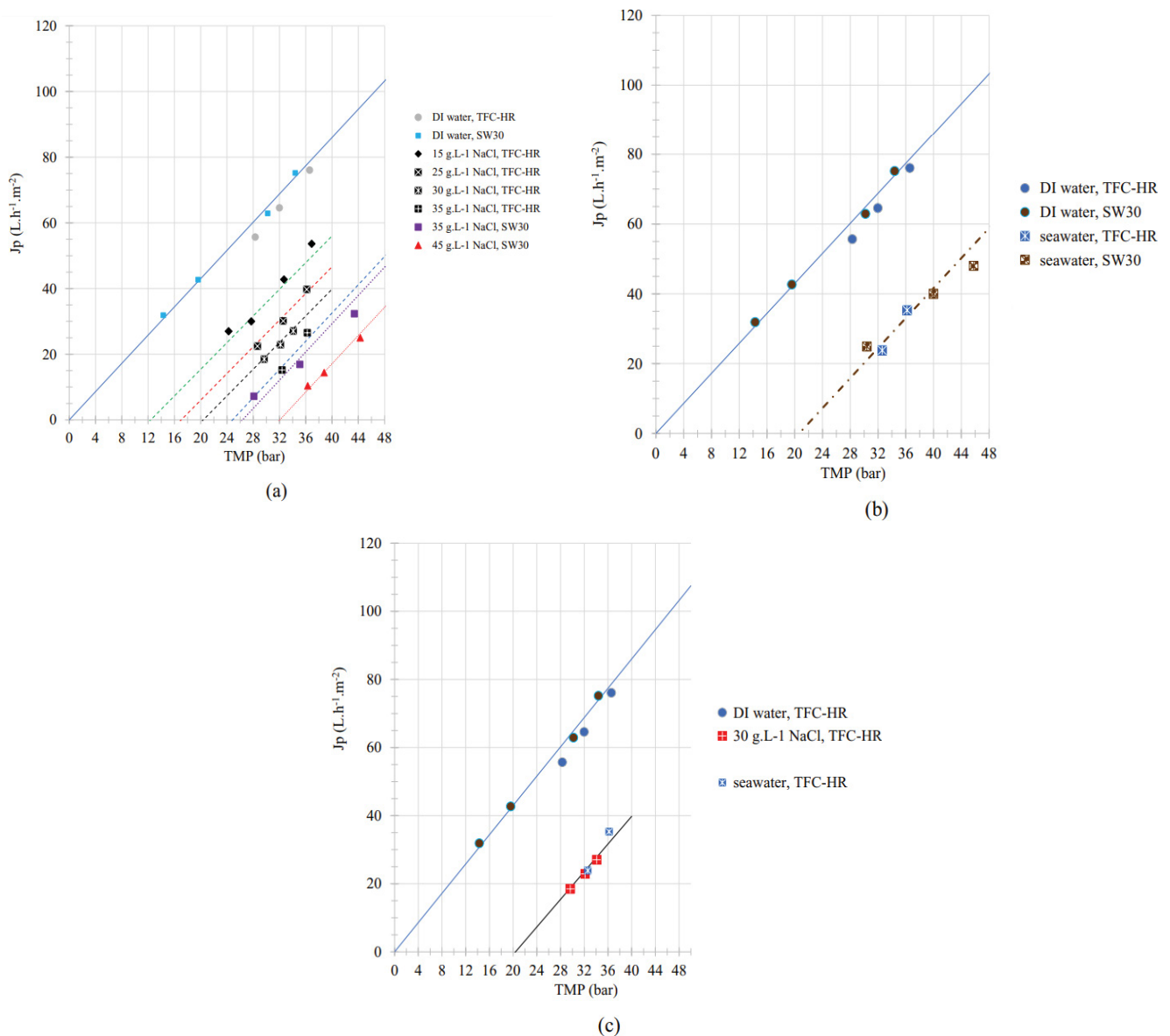


Fig. 11. Permeate flux (J_p) vs. applied transmembrane pressure (TMP) of TFC-HR (30°C, 0.5 $\text{m}\cdot\text{s}^{-1}$) and SW30 (25°C, 2.5 $\text{m}\cdot\text{s}^{-1}$): (a) in DI water and 15–45 $\text{g}\cdot\text{L}^{-1}$ NaCl at natural neutral pH, (b) in DI water and synthetic seawater (pH 8.2) and (c) in DI water, 30 $\text{g}\cdot\text{L}^{-1}$ NaCl (neutral pH) and synthetic seawater (pH = 8.2).

that were at neutral pH, regardless of the membrane, the pH remained neutral either in the retentate and in the permeate. However, in the synthetic seawater, the pH was more acid in the permeate than in the retentate with the TFC-HR membrane, suggesting a negative rejection of the proton. Such permeate acidification is a well-known phenomenon in seawater RO generally attributed to the complex $\text{CO}_2/\text{HCO}_3^-$ balance and not to a transfer mechanism based on the Donnan partition at the membrane wall as in aqueous nanofiltration. However, with the SW30, the pH difference between the retentate and the permeate was not significant, highlighting that further experiments are needed to have a better understanding of the origin of the differences between the two membranes' behavior.

3.4. RO of charged organic molecules

The impact of the seawater matrix on the rejection of small charged organic solutes of close molecular weight was studied. RO was achieved at two selected pHs, either 4.5–4.8/5.2 (natural pH of the Thiamine-Tropaeolin O solutions with or without NaCl addition or pH = 8.2 (synthetic seawater). Accordingly, Tropaeolin O was mainly a monovalent (acid pH) or a divalent (seawater) anion while Thiamine was mainly a divalent (acid pH) or a monovalent (seawater) cation. It can be noticed that for a given compound, the higher its net charge is, the more hydrophilic is the component.

With respect to their zeta potential, the two virgin membranes were more or less negatively charged for these

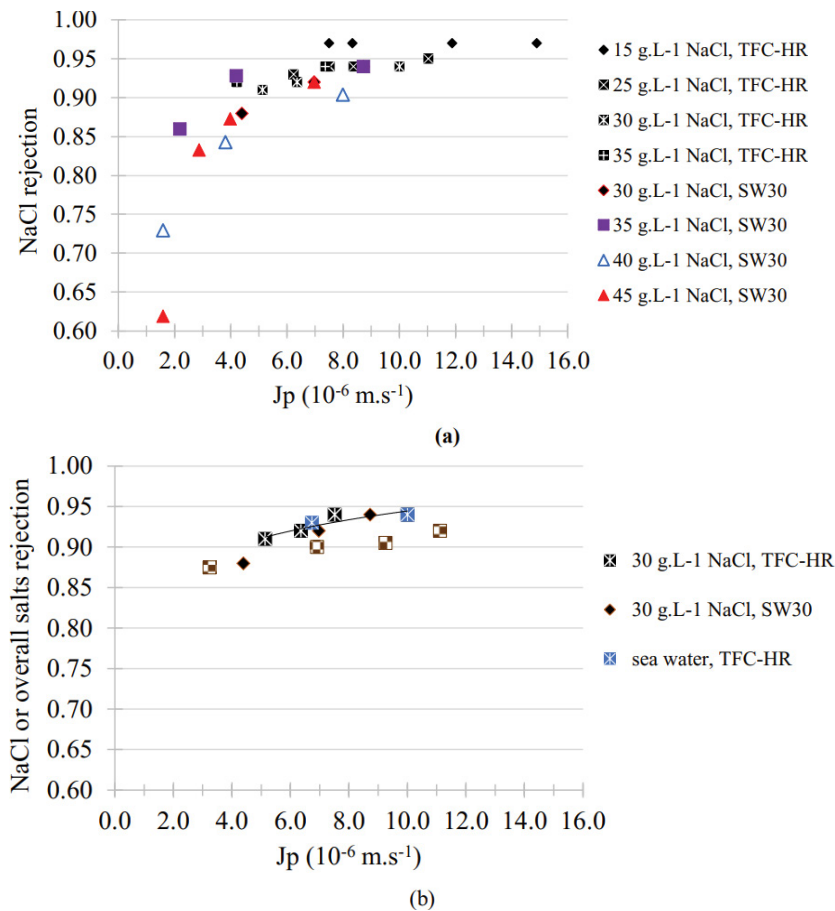


Fig. 12. Rejections by TFC-HR (30–36 bar TMP range, 30°C, 0.5 m s⁻¹) and SW30 (25–46 bar TMP range, 25°C, 2.5 m s⁻¹): (a) NaCl rejection at neutral pH for 15–45 g L⁻¹ NaCl solutions and (b) 30 g L⁻¹ NaCl at neutral pH and overall seawater salts (pH 8.2) from conductivity measurements.

Table 7

Comparison of NaCl and synthetic seawater at plateau value of rejection during RO by TFC-HR (32–36 bar TMP range, 30°C, 0.5 m s⁻¹) and SW30 (30–46 bar TMP range, 25°C, 2.5 m s⁻¹)

Membrane	TFC-HR				SW30	
	NaCl		Synthetic seawater		NaCl	
	30 g L ⁻¹	35 g L ⁻¹			30 g L ⁻¹	35 g L ⁻¹
$\Delta\pi_0$ (bar)	21	25	21	21	25	24–26
	0.93	0.93	0.934	0.91	0.94	0.93
Salts' rejection ^a (TMP range, bar)	±0.02 (32–36)	±0.02 (32–36)	±0.004 (32–36)	±0.01 (30–40)	0.01 (35–46)	0.06 (35–44)
pH feed/retentate	6.69	6.68	8.20 ± 0.07	8.41 ± 0.09	6.1 ± 0.7	5.75
pH permeate	6.52	6.45	6.04 ± 0.01	8.66 ± 0.11	7.1 ± 0.7	6.77
H ₃ O ⁺ rejection	≈0	≈0	-144	≈0	0.90	0.90
OH ⁻ rejection	≈0	≈0	0.99	≈0	-9	-10

^aby conductimetry for synthetic seawater

pHs. Thus, the fouling was expected to be different due to attraction or repulsion between the membrane and Thiamine or Tropaeolin O, respectively, even if concentrations were low ($0.5 \times 10^{-3} \text{ mol L}^{-1}$). What was the impact of solutes' charges

on the rejections? Particularly in 30 g L⁻¹ NaCl and synthetic seawater having a high ionic strength of 0.5–0.6 mol L⁻¹, respectively, were electrostatic interactions sufficiently screened to cancel every associated impact?

3.4.1. Tropaeolin O (mono or divalent anion)

The azo dye was filtered in water and in water/ethanol.

3.4.1.1. In water

Tropaeolin O was filtered in water with the two membranes (Figs. 13 and 14).

Fig. 13 shows RO by TFC-HR of Tropaeolin O in a single solution at two different pHs (5.2 and 6.8) leading either to a monovalent or mainly divalent anion. Regardless of the pH, no reduction of the water flux was evidenced

(Fig. 13a). This is in good agreement with both the low concentration and the occurrence of electrostatic repulsions between the negatively charged dye and the negatively charged virgin RO membrane. The pH of the permeate was close to that of the retentate (Table 8). When adding either 30 g L⁻¹ NaCl (pH = 4.8) or seawater (pH = 8.2), the flux was clearly decreased and controlled by the salt (Fig. 13b). At $J_p = 0$, $\Delta\pi_0 = 22$ bar was similar to the extrapolated value for the same solutions without any dye dissolved in (Table 7).

In a single solution (Fig. 13c, Table 8), the Tropaeolin O rejection was higher when the dye was the more negatively

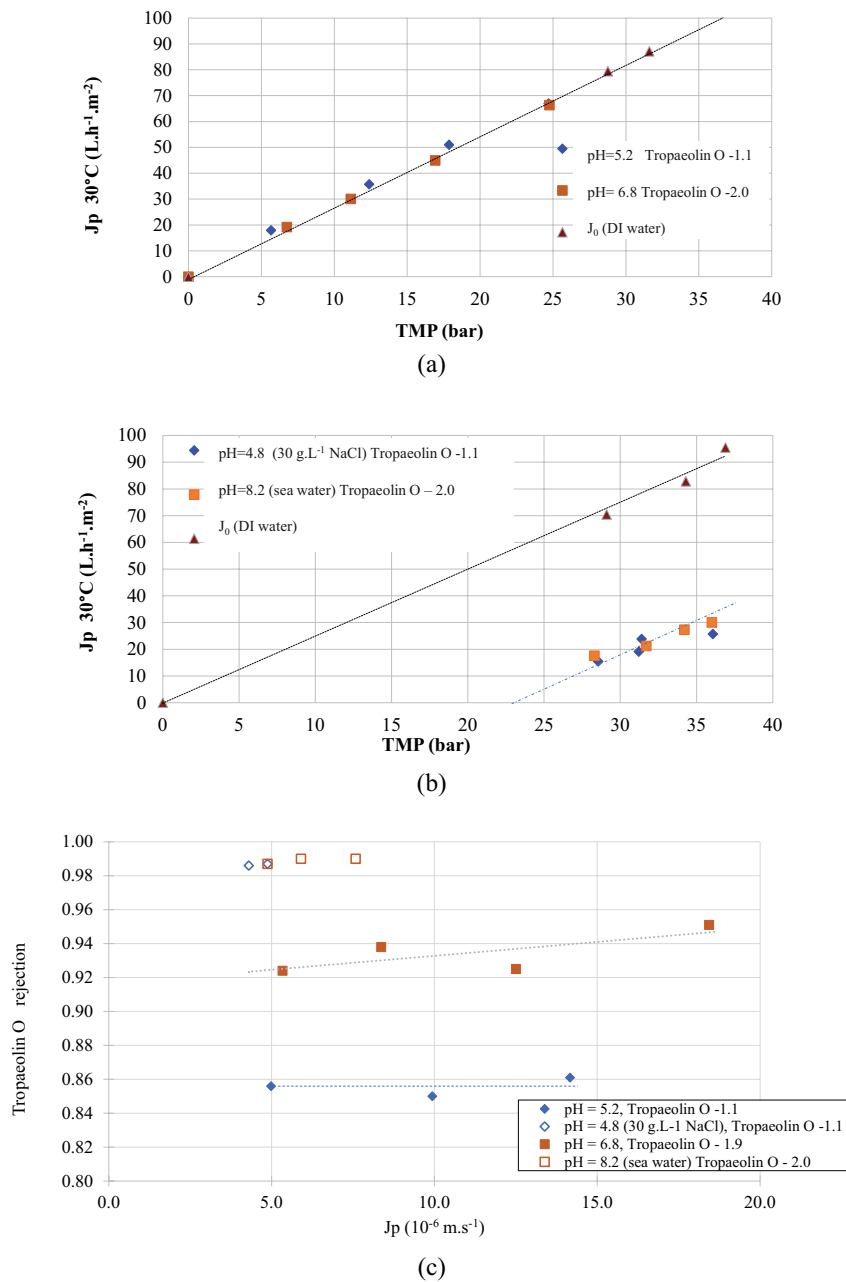


Fig. 13. Tropaeolin O (0.5 mM) RO by TFC-HR membrane at 30°C, 0.5 m s⁻¹. (a) Flux in single Tropaeolin O solution at various pH, (b) flux for Tropaeolin O in 30 g L⁻¹ NaCl (pH = 4.8) and seawater (pH = 8.2) and (c) Tropaeolin O rejection at acid pH (single or NaCl) and neutral-alkaline pH (single or seawater).

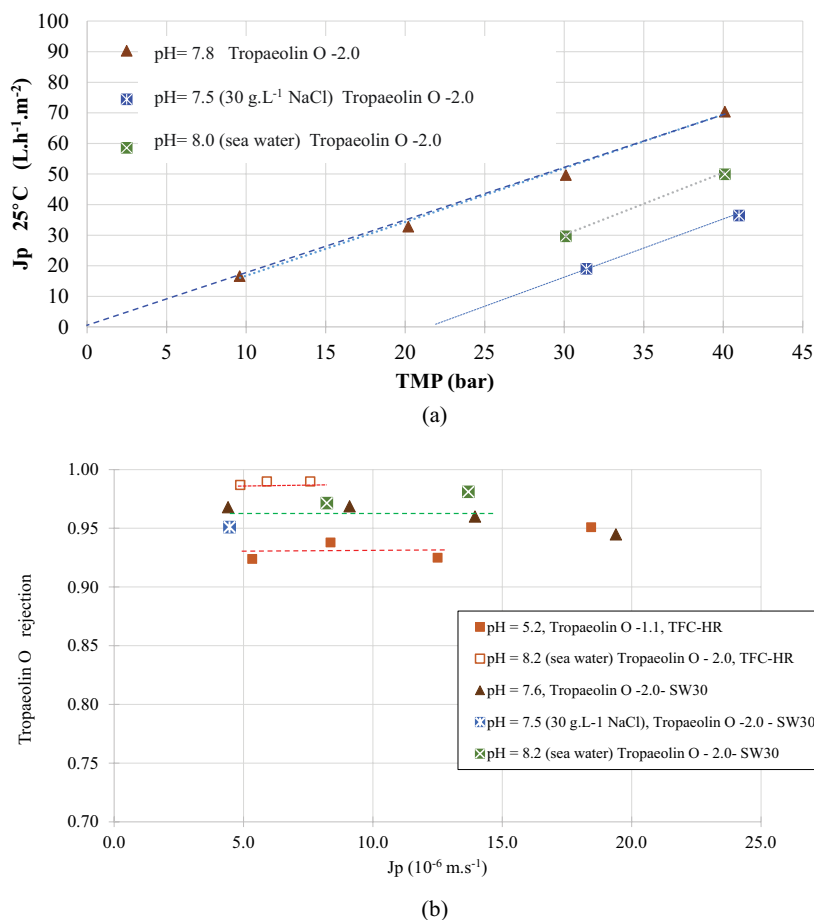


Fig. 14. Tropaeolin O (0.5 mM, divalent anion) RO by the SW30 membrane at 25°C, 2.5 m s⁻¹ (a) flux and (b) rejection.

charged (and simultaneously in its more hydrophilic form) suggesting an impact of electrostatic repulsions between the negative TFC-HR membrane and its monovalent/divalent co-ion (it can be noticed that with or without any dye adsorption, the active membrane would remain negatively charged as the virgin TFC-HR). The pH of the permeate was close to that of the retentate (Table 8).

At pH ≥ 6.5 , in presence of either 30 g L⁻¹ NaCl or synthetic seawater, the Tropaeolin O rejection increased. At first sight (discussion section), this trend appeared likely due to the Tropaeolin O charge increase whereas the salt content seemed to have no impact on the rejection even if the ionic strength was significantly increased from a few mM in a single solution to 0.5–0.6 M in slated solutions (Table 8). Simultaneously, the rejection of salts seemed not affected by the presence of Tropaeolin O. While the pH of both permeate and retentate remained close in NaCl, in seawater the permeate acidification was lower in presence of Tropaeolin O than without it (Table 8).

Similarly, RO of divalent Tropaeolin O (pH ≥ 7.4) was achieved with the SW30 membrane (Fig. 14, Table 9). The Tropaeolin O rejection was roughly the same in a single solution and synthetic seawater confirming the TFC-HR results on the absence of impact on the dye rejection associated with the salt presence. Contrary to what happened with the TFC-HR no acidification of the permeate was

evidenced during the RO of the synthetic seawater by the SW30 membrane. Moreover, the permeate was more alkaline in 30 g L⁻¹ NaCl with or without the dye dissolved in. These results suggest that the difference in the two membranes' composition and initial zeta potential might have an impact on selectivity.

3.4.1.2. In water/ethanol (TFC-HR membrane)

The objective here was to evidence if the transfer of Tropaeolin O (0.5 mM, stokes radius ≈ 0.5 nm, Table 5) can be modified, for instance, due to cooperative effects, in presence of a large amount of other small organic solutes able to partially cross the RO membrane. Ethanol (stokes radius ≈ 0.3 [43]–0.4 nm, Tables 3 and 5) was selected as a unique compound aiming at modeling a concentrated mixture of small organics.

Ethanol was also selected because it can act as a solvent that was fully miscible with water. Their mixture created a background solvent (BGS) different from water when dealing with the density and the viscosity increase and the dielectric constant decrease with the ethanol content increase [44–47]. Moreover, ethanol affinity toward the polymer membrane is better than that of DI water with respect to its less hydrophilic character. To increase ethanol amount induced an increase in the BGS affinity toward

Table 8

Tropaeolin O (0.5 mM, anion) reverse osmosis by TFC-HR membrane at 30°C, 0.5 m s⁻¹ in the 28–36 bar applied transmembrane pressure range (plateau value of rejection)

Tropaeolin O	Monovalent		Mainly divalent		Divalent	
	Single	30 g L ⁻¹ NaCl		Single	Seawater	
	Tropaeolin O	With Tropaeolin O	Without Tropaeolin O	Tropaeolin O	Without Tropaeolin O	With Tropaeolin O
Feed pH	5.2	6.5	6.7	6.8	8.2	8.3
NaCl rejection	–	0.93 ± 0.01	0.93 ± 0.02	–	–	–
Salts rejection ^a	–	–	–	–	0.93 ± 0.01	0.94 ± 0.01
Tropaeolin O rejection	0.86 ± 0.01	0.98 ± 0.01	–	0.94 ± 0.01	–	0.99 ± 0.01
pH retentate	5.24	6.52 ± 0.08	6.69	6.79	8.20 ± 0.07	8.29 ± 0.05
pH permeate	5.97	6.75 ± 0.09	6.52	6.30	6.04 ± 0.01	7.49 ± 0.1
H ₃ O ⁺ rejection	≈0	≈0	≈0	≈0	–144	–5
OH ⁻ rejection	≈0	≈0	≈0	≈0	0.99	0.84

^aby conductimetry for synthetic seawater

Table 9

Tropaeolin O (0.5 mM) reverse osmosis by SW30 membrane at 25°C, 2.5 m s⁻¹ in the 30–45 bar applied transmembrane pressure range (plateau value of rejection)

Tropaeolin O	Divalent anion				
	Tropaeolin O	30 g L ⁻¹ NaCl		Seawater	
		Without Tropaeolin O	With Tropaeolin O	Without Tropaeolin O	With Tropaeolin O
Feed pH	7.8	6.1	7.4	8.4	8.3
NaCl rejection (30–40 bar)	–	0.94 ± 0.01	0.92 ± 0.02	–	–
Salts rejection (35–45 bar)	–	–	–	0.91 ± 0.01	0.94 ± 0.01
Tropaeolin O rejection (30–40 bar)	0.96 ± 0.01	–	0.94 ± 0.01	–	0.976 ± 0.003
pH retentate	7.6 ± 0.3	6.1 ± 0.7	7.4 ± 0.4	8.4 ± 0.1	8.0 ± 0.1
pH permeate	8.1 ± 0.6	7.1 ± 0.7	8.4 ± 0.3	8.6 ± 0.1	8.3 ± 0.2
H ₃ O ⁺ rejection	0.65	0.90	0.89	≈0	≈0
OH ⁻ rejection	–2	–9	–8	≈0	≈0

the polyamide membrane with respect to their respective Hansen–Hildebrand parameter as reported in [32,48].

Tropaeolin O was filtered at natural pH = 4.8 and 20 bar with the TFC-HR membrane in water/ethanol mixtures either 90/10 or 70/30 v/v. To avoid any salt precipitation, NaCl was added at 0.1 mol L⁻¹ (5.85 g L⁻¹) which would be a sufficiently high concentration to efficiently screen electrostatic interactions, if any, even if it can be guessed that they were not fully canceled.

Compared to water, the fluxes decreased in water/ethanol and were controlled by the viscosity and the osmotic pressure due to ethanol. The presence of Tropaeolin O with or without NaCl had no significant impact on the flux. It was checked that the ethanol rejection remained low and roughly constant over the whole range of experiences.

Fig. 15 shows that Tropaeolin O was better transmitted in presence of ethanol than in DI water. In presence of NaCl, the rejection decreased. It seemed that in presence of ethanol, a competition was established between the membrane

and the BGS with respect to the organic solute affinity (Table 5). The consequence was a better transmission of the dye compound toward the permeate. This can be considered as a synergetic effect of the mixture of Tropaeolin O and ethanol, highlighting the interest in studying mixtures of organics with an overall high concentration.

3.4.2. Thiamine (mono or divalent cation)

Thiamine was only filtered with the TFC-HR in the 5–36 bar range (Fig. 16, Table 10).

At pH = 4.5 the flux in water and in a single Thiamine solution were the same, while the flux decreased significantly at pH 6.4 (Fig. 16a). The permeate flux was similar in DI water and when simultaneously Thiamine was mainly a divalent cation (Thiamine^{+1.7}, pH 4.5) and TFC-HR membrane was negatively charged (virgin membrane zeta potential ≈ –15 mV, Fig. 8). On the contrary, when Thiamine was a monovalent cation (Thiamine^{+0.9}, pH 6.4) and the virgin

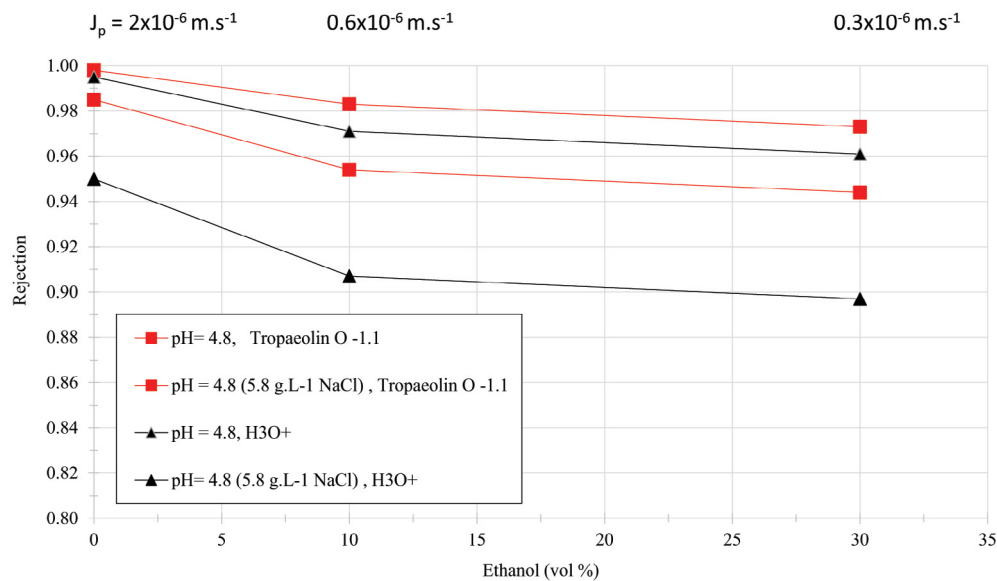


Fig. 15. Tropaeolin O (0.5 mM, monovalent anion) RO at 20 bar by TFC-HR membrane at 18°C, 0.8 m s⁻¹ in various water/ethanol mixtures from 100/0 to 70/30 v/v.

Table 10

Thiamine (0.5 mM, cation) reverse osmosis by TFC-HR membrane at plateau value of rejection during RO (29–36 bar TMP range, 30°C, 0.5 m s⁻¹)

Thiamine	Mainly divalent			Monovalent cation		
	Single	30 g L ⁻¹ NaCl		Single	Seawater	
	Thiamine	With Thiamine	Without Thiamine	Thiamine	Without Thiamine	With Thiamine
Feed pH	4.5	4.5	6.7	6.4	8.2	8.3
NaCl rejection	–	0.91 ± 0.02	0.93 ± 0.02	–	–	–
Salts rejection	–	–	–	–	0.934 ± 0.004	0.94 ± 0.02
Thiamine rejection	0.95 ± 0.01	0.95 ± 0.01	–	0.95 ± 0.01	–	0.96 ± 0.01
pH retentate	4.00 ± 0.07	4.45 ± 0.04	6.69 ± 0.05	6.44 ± 0.4	8.20 ± 0.07	8.30 ± 0.04
pH permeate	4.59 ± 0.05	4.75 ± 0.07	6.52 ± 0.05	5.75 ± 0.2	6.04 ± 0.01	7.34 ± 0.13
H ₃ O ⁺ rejection	≈0	≈0	≈0	–4	–144	–8
OH ⁻ rejection	≈0	≈0	≈0	0.80	0.99	0.89

membrane was a little bit more negatively charged (zeta potential ≈ –20 mV, Fig. 8) the flux significantly decreased. This result appeared counter-intuitive at first sight if the fouling was managed by electrostatic interactions. However, it appeared logical if the fouling was mainly the consequence of hydrophobic solute/membrane interactions (as suggested from adsorption experiments achieved with Tropaeolin O, Section 3.2 – Irreversible adsorption of Tropaeolin O on TFC-HR and SW30 membranes) because Thiamine^{+1.7} is more hydrophilic than Thiamine^{+0.9} due to their respective charge.

Fig. 16b shows the RO of Thiamine mixed either with NaCl at 30 g L⁻¹, pH = 4.5 or synthetic seawater (pH 8.2). In both cases, the permeate flux was clearly controlled by the salt. At $J_p = 0$, $\Delta\pi_0 = 21$ bar as already observed for the same solutions without any Thiamine dissolved in (Table 7).

Fig. 16c compares the Thiamine rejections vs. flux. In a single solution, the rejection ranged from 0.92 to 0.96 and

varied linearly with the flux. The more charged (and hydrophilic) was the Thiamine the less it was rejected. In presence of salts, either 30 g L⁻¹ NaCl or seawater, Thiamine rejection increased compared to single solutions, however, no significant difference was evidenced for the two pHs.

Thiamine, either in monovalent or divalent form, seemed to have no impact on salts' rejection, as was evidenced from conductivity measurements. However, the acidification of the seawater permeate was lower with Thiamine than without Thiamine (Table 10).

4. Discussion: comparison Tropaeolin O/Thiamine in water

Tropaeolin O and Thiamine were selected at the start because of their close molecular weight and their opposite charges. Moreover, with respect to $\log K_{ow}$, their

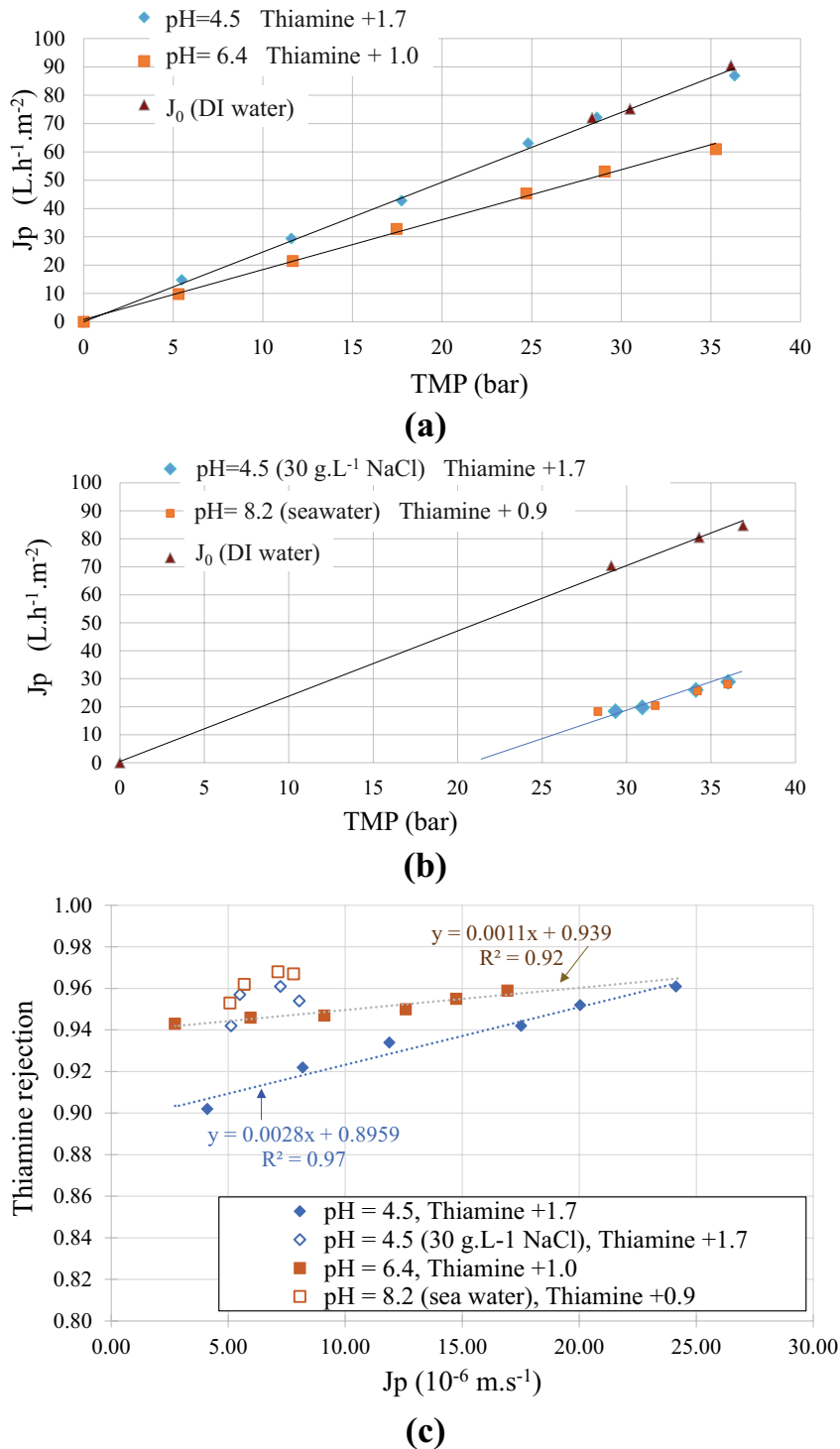


Fig. 16. Thiamine (0.5 mM, cation) RO by TFC-HR membrane at 30°C, 0.5 m s⁻¹. (a) Flux in single solution at pH 4.5 and 6.4, (b) flux in 30 g L⁻¹ NaCl pH 4.5 and seawater pH 8.2 and (c) rejection.

hydrophobicity is close, but it must be underlined that this value does not take into account the variation of the solute charges. Finally, their respective affinity toward the two RO membranes appeared similar from the Hansen–Hildebrand solubility parameters (Table 5); but once again such calculations did not account for charge variation.

The variation of the average net charge of the two solutes was plotted vs. the pH and compared to the zeta potential of the two virgin membranes remaining negatively charged over the whole studied pH range (Fig. 17). When increasing the pH, the Tropaeolin O negative net charge increases whereas the positive net charge

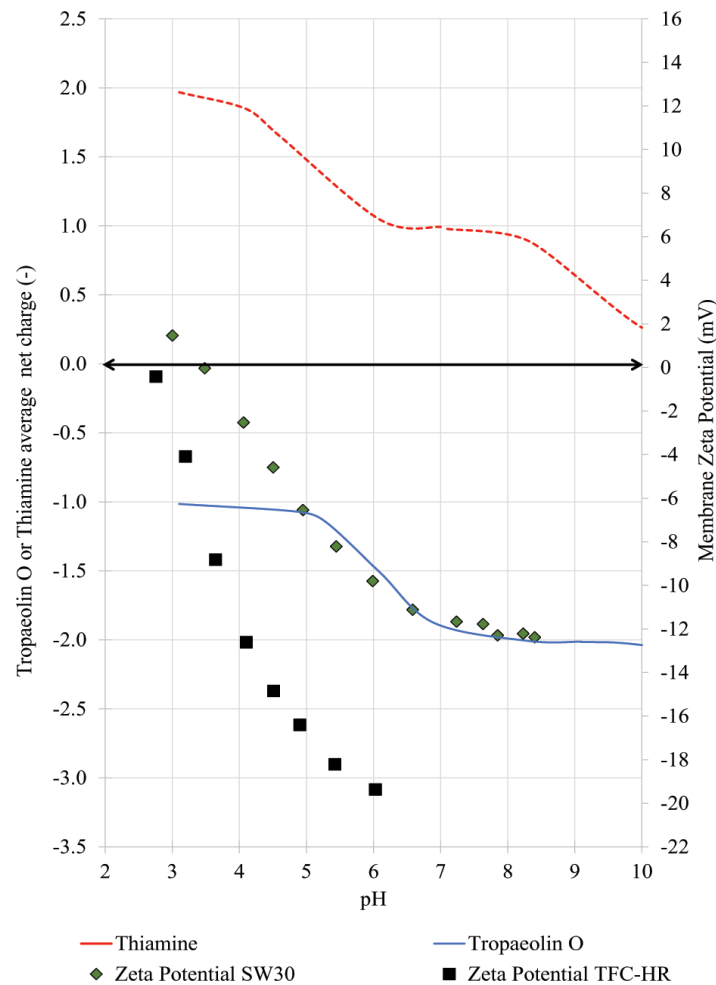


Fig. 17. Comparison of the average net charge of Tropaeolin O and zeta potential of the two membranes (in 1 mmol L⁻¹ KCl).

of Thiamine decreases. Simultaneously, in absence of charge screening by a high amount of added salts, Tropaeolin O hydrophobicity increases whereas Thiamine hydrophobicity increases with the pH. However, when adding a high amount of salts (but how much exactly?), the screening of the charges would be efficient and consequently, the hydrophobicity of each solute would be maximum, regardless of the pH.

For a better fundamental comprehension of mechanisms, the comparison must be achieved at constant permeate flux. $J_p = 5.10^{-6} \text{ m s}^{-1}$ was selected as depicted in Fig. 18. First of all, regardless of the organic solute and its physicochemical environment, the rejection was neither full nor in the relative order of the MW.

In a single solution, Tropaeolin O rejection by the TFC-HR membrane was increased when increasing the pH and consequently its negative charge. Such behavior appeared in good agreement with repulsive electrostatic interactions between the membrane and its co-ion.

In a single solution, Thiamine rejection by the TFC-HR was decreased when the pH decreased and consequently, its net charge increased. Such behavior appeared in good agreement with attractive electrostatic interactions between the membrane and its counter-ion.

In 30 g L⁻¹ NaCl or seawater, the ionic strength was in the 0.5–0.6 M range, and electrostatic interactions might be significantly decreased. However, rejections of the most charged form of Tropaeolin O by the TFC-HR membrane were increased with respect to either the monovalent anion or the divalent anion without any added salt. Similarly, rejections of Thiamine increased, regardless of its charge.

As the electrostatic interactions between the charged membrane and its co-ion (Tropaeolin O) or counter-ion (Thiamine) might be less efficient due to the screening induced by the ionic strength, the Tropaeolin O rejection might decrease due to a decrease of repulsion whereas that of Thiamine might increase due to decrease of attraction. The results shown in Fig. 18 are not in line with this comment and show that the explanation of the rejection variation was not only due to membrane/solute electrostatic interactions. It seems more logical to draw that the rejections were improved when simultaneously the hydrophobicity of solute and membrane was increased with respect to a significant amount of salt addition. The variation of the Tropaeolin O rejection by the SW30 membrane with or without added salt is in good agreement with this explanation.

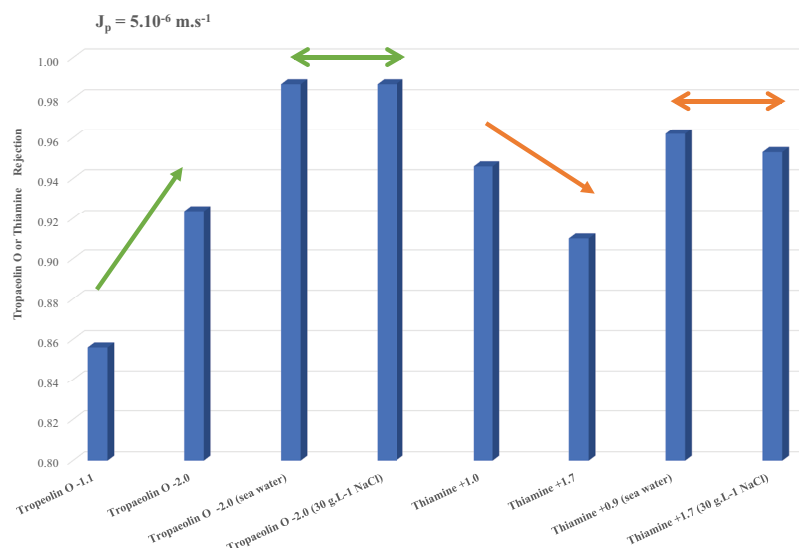


Fig. 18. Comparison of Tropaeolin O (293 g mol^{-1} , anion) and Thiamine (265 g mol^{-1} , cation) rejection by the TFC-HR membrane at $J_p = 5.10^{-6} \text{ m s}^{-1}$.

5. Conclusions

In this study, we have selected a commercial mixture of sea salts (Instant Ocean) and shown that its behavior during RO either by a TFC-HR or a SW30 membrane was close to that of $30 \text{ g L}^{-1} \text{ NaCl}$ with respect to the overall salt rejection as it can be studied without any selectivity from conductivity measurements.

Then, we have selected two organics of similar molecular weight and close hydrophobicity, one being negatively charged (Tropaeolin O, azo dye) and the other positively charged (Thiamine) in order to study the impact of the seawater matrix on their respective transfer through polyamide membranes.

The transfer of the two organic compounds was more fundamentally studied with the TFC-HR membrane. By playing simultaneously on the monovalent/divalent charge and on the hydrophilic/hydrophobic balance of the solutes, thanks to the pH and the ionic strength of the physico-chemical environment, the rejections were changed.

At constant flux $J_p = 5.10^{-6} \text{ m s}^{-1}$, the more hydrophobic form of a given solute, obtained by adding salts (either NaCl or seawater), was systematically more rejected than the hydrophilic ones (regardless of their monovalent/divalent co-ion or counter-ion form).

In our future work, one issue that absolutely must be addressed is that of mixtures of small organics (pollutants), the molecular weight of which being close to $250\text{--}300 \text{ g mol}^{-1}$, as contrary to current thought they are able to cross the RO membranes. With respect to the impact of ethanol addition in water shown in this paper, it is probably necessary to distinguish between (i) mixtures of organics that only lead to an overall concentration increase with a possible impact on the amount adsorbed at the membrane wall, and (ii) those, like ethanol, that could induce a better transfer due to an increased affinity of the organic solute for the background solvent when compared to water. In our opinion, the first case is widely studied in many papers for solutes with

$\text{MW} \leq 150 \text{ g mol}^{-1}$, but not the second one that makes the junction between water and organic solvent filtration either in nanofiltration or reverse osmosis.

Acknowledgments

The authors acknowledge Prof. Anthony Szymczyk, Univ Rennes ISCR, for his help and advice in the streaming potential/current measurements.

OS acknowledges the CEDOC program (France-Morocco cooperation) & Campus France for a Ph.D. grant (2017/08 100).

FZC acknowledges Eiffel & Campus France for the Ph.D. grant n° EIFFEL-DOCTORAT 2020/n°P757215H.

AB acknowledges Univ. Mostaganem for a residence grant at ISCR.

References

- [1] M. Elimelech, W.A. Phillip, The future of seawater desalination: energy, technology, and the environment, *Science*, 333 (2011) 712–717.
- [2] C. Fritzmann, J. Löwenberg, T. Wintgens, T. Melin, State-of-the-art of reverse osmosis desalination, *Desalination*, 216 (2007) 1–76.
- [3] E. Jones, M. Qadir, M.T.H. van Vliet, V. Smakhtin, S.-m. Kang, The state of desalination and brine production: a global outlook, *Sci. Total Environ.*, 657 (2019) 1343–1356.
- [4] I. Ullah, M.G. Rasul, Recent developments in solar thermal desalination technologies: a review, *Energies*, 12 (2018) 119, doi: 10.3390/en12010119.
- [5] K. Elsaid, E.T. Sayed, M.A. Abdelkareem, A. Baroutaji, A.G. Olabi, Environmental impact of desalination processes: mitigation and control strategies, *Sci. Total Environ.*, 740 (2020) 140125, doi: 10.1016/j.scitotenv.2020.140125.
- [6] H. Miyakawa, M. Maghram Al Shaia, T.N. Green, Y. Ito, Y. Sugawara, M. Onishi, Y. Fusaoka, M. Farooque Ayumantakath, A. Saleh Al Amoudi, Reliable seawater Ro operation with high water recovery and no-chlorine/No-Sbs dosing in Arabian Gulf, Saudi Arabia, *Membranes*, 11 (2021) 141, doi: 10.3390/membranes11020141.

- [7] K.E. Murray, S.M. Thomas, A.A. Bodour, Prioritizing research for trace pollutants and emerging contaminants in the freshwater environment, *Environ. Pollut.*, 158 (2010) 3462–3471.
- [8] R.P. Schwarzenbach, B.I. Escher, K. Fenner, T.B. Hofstetter, C. Annette Johnson, U. von Gunten, B. Wehrli, The challenge of micropollutants in aquatic systems, *Science*, 313 (2006) 1072–1077.
- [9] Y.J. Lim, K. Goh, M. Kurihara, R. Wang, Seawater desalination by reverse osmosis: current development and future challenges in membrane fabrication – a review, *J. Membr. Sci.*, 629 (2021) 119292, doi: 10.1016/j.memsci.2021.119292.
- [10] J.G. Wijmans, R.W. Baker, The solution–diffusion model: a review, *J. Membr. Sci.*, 107 (1995) 1–21.
- [11] M. Miettton-Peuchot, V. Milisic, P. Noilet, Grape must concentration by using reverse osmosis. Comparison with chaptalization, *Desalination*, 148 (2002) 125–129.
- [12] C. Sagne, C. Fargues, R. Lewandowski, M.-L. Lameloise, M. Gavach, M. Decloux, A pilot scale study of reverse osmosis for the purification of condensate arising from distillery stillage concentration plant, *Chem. Eng. Process. Process Intensif.*, 49 (2010) 331–339.
- [13] Q. Ramsey, Q. Yang, I. Fisk, C. Ayed, R. Ford, Assessing the sensory and physicochemical impact of reverse osmosis membrane technology to dealcoholize two different beer styles, *Food Chem.: X*, 10 (2021) 100121, doi: 10.1016/j.fochx.2021.100121.
- [14] C. Bellona, J.E. Drewes, P. Xu, G. Amy, Factors affecting the rejection of organic solutes during NF/RO treatment—a literature review, *Water Res.*, 38 (2004) 2795–2809.
- [15] L.F. Greenlee, D.F. Lawler, B.D. Freeman, B. Marrot, P. Moulin, Reverse osmosis desalination: water sources, technology, and today's challenges, *Water Res.*, 43 (2009) 2317–2348.
- [16] H. Bouzid, M. Rabiller-Baudry, Z. Derriche, N. Bettahar, Fluxes in reverse osmosis of model acidic and alkaline transient effluents issued from skim milk filtration, *Desal. Water Treat.*, 43 (2012) 52–62.
- [17] J. Jaime Sadhwani Alonso, N. El Kori, N. Melián-Martel, B. Del Río-Gamero, Removal of ciprofloxacin from seawater by reverse osmosis, *J. Environ. Manage.*, 217 (2018) 337–345.
- [18] N. Al-Bastaki, Removal of methyl orange dye and Na_2SO_4 salt from synthetic waste water using reverse osmosis, *Chem. Eng. Process. Process Intensif.*, 43 (2004) 1561–1567.
- [19] L. Wang, C. Albasi, V. Faucet-Marquis, A. Pfohl-Leszkwicz, C. Dorandeu, B. Marion, C. Causserand, Cyclophosphamide removal from water by nanofiltration and reverse osmosis membrane, *Water Res.*, 43 (2009) 4115–4122.
- [20] M. Xie, L.D. Nghiem, W.E. Price, M. Elimelech, Comparison of the removal of hydrophobic trace organic contaminants by forward osmosis and reverse osmosis, *Water Res.*, 46 (2012) 2683–2692.
- [21] J. Heo, L.K. Boateng, J.R.V. Flora, H. Lee, N. Her, Y.-G. Park, Y. Yoon, Comparison of flux behavior and synthetic organic compound removal by forward osmosis and reverse osmosis membranes, *J. Membr. Sci.*, 443 (2013) 69–82.
- [22] E. Dražević, K. Košutić, M. Svalina, J. Catalano, Permeability of uncharged organic molecules in reverse osmosis desalination membranes, *Water Res.*, 116 (2017) 13–22.
- [23] M. Ding, A. Szymczyk, F. Goujon, A. Soldera, A. Ghoufi, Structure and dynamics of water confined in a polyamide reverse-osmosis membrane: a molecular-simulation study, *J. Membr. Sci.*, 458 (2014) 236–244.
- [24] H. Yan, X. Miao, J. Xu, G. Pan, Y. Zhang, Y. Shi, M. Guo, Y. Liu, The porous structure of the fully-aromatic polyamide film in reverse osmosis membranes, *J. Membr. Sci.*, 475 (2015) 504–510.
- [25] F. Pacheco, R. Sougrat, M. Reinhard, J.O. Leckie, I. Pinnau, 3D visualization of the internal nanostructure of polyamide thin films in RO membranes, *J. Membr. Sci.*, 501 (2016) 33–44.
- [26] L. Lin, R. Lopez, G.Z. Ramon, O. Coronell, Investigating the void structure of the polyamide active layers of thin-film composite membranes, *J. Membr. Sci.*, 497 (2016) 365–376.
- [27] M.M. Kłosowski, C.M. McGilvery, Y. Li, P. Abellan, Q. Ramasse, J.T. Cabral, A.G. Livingston, A.E. Porter, Micro-to nano-scale characterisation of polyamide structures of the SW30HR RO membrane using advanced electron microscopy and stain tracers, *J. Membr. Sci.*, 520 (2016) 465–476.
- [28] <https://www.aquaportal.com/definition-7158-eau-de-mer-naturelle.html>
- [29] M.J. Atkinson, C. Bingman, Elemental composition of commercial sealants, *J. Aquaculture Aquat. Sci.*, 8 (1997) 39–43.
- [30] V.O. Doroshuk, S.A. Kulichenko, S.O. Lelyushok, The influence of substrate charge and molecular structure on interphase transfer in cloud point extraction systems, *J. Colloid Interface Sci.*, 291 (2005) 251–255.
- [31] https://www.chemsrc.com/en/cas/70-16-6_585810.html
- [32] T.V.N. Nguyen, L. Paugam, P. Rabiller, M. Rabiller-Baudry, Study of transfer of alcohol (methanol, ethanol, isopropanol) during nanofiltration in water/alcohol mixtures, *J. Membr. Sci.*, 601 (2020) 117907, doi: 10.1016/j.memsci.2020.117907.
- [33] G. Socrates, *Infrared and Raman Characteristic Group Frequencies: Tables and Charts*, John Wiley & Sons, Hoboken, New Jersey, USA 2004.]
- [34] <https://www.lenntech.com/Data-sheets/Koch-Fluid-Systems-TFC-4820-HR-L.pdf>
- [35] L. Le Petit, M. Rabiller-Baudry, R. Touin, R. Chataignier, P. Thomas, O. Connan, R. Périon, Efficient and rapid multiscale approach of polymer membrane degradation and stability: application to formulation of harmless non-oxidative biocide for polyamide and PES/PVP membranes, *Sep. Purif. Technol.*, 259 (2021) 118054, doi: 10.1016/j.seppur.2020.118054.
- [36] https://www.lenntech.com/feed-back/feed-back_uk.htm?ref_title=Filmtec/Dow-Filmtec-SW30-4040.pdf
- [37] I. Sutzkover, D. Hasson, R. Semiat, Simple technique for measuring the concentration polarization level in a reverse osmosis system, *Desalination*, 131 (2000) 117–127.
- [38] E.M. Van Wagner, A.C. Sagle, M.M. Sharma, B.D. Freeman, Effect of crossflow testing conditions, including feed pH and continuous feed filtration, on commercial reverse osmosis membrane performance, *J. Membr. Sci.*, 345 (2009) 97–109.
- [39] Y. Hanafi, P. Loulergue, S. Ababou-Girard, C. Meriadec, M. Rabiller-Baudry, K. Baddari, A. Szymczyk, Electrokinetic analysis of PES/PVP membranes aged by sodium hypochlorite solutions at different pH, *J. Membr. Sci.*, 501 (2016) 24–32.
- [40] R.F. Fedors, A method for estimating both the solubility parameters and molar volumes of liquids, *Polym. Eng. Sci.*, 14 (1974) 147–154.
- [41] M. Rabiller-Baudry, A. Bouzin, C. Hallery, J. Girard, C. Leperoux, Evidencing the chemical degradation of a hydrophilised PES ultrafiltration membrane despite protein fouling, *Sep. Purif. Technol.*, 147 (2015) 62–81.
- [42] Q. Li, J. Song, H. Yu, Z. Li, X. Pan, B. Yang, Investigating the microstructures and surface features of seawater RO membranes and the dependencies of fouling resistance performances, *Desalination*, 352 (2014) 109–117.
- [43] B. Van der Bruggen, J. Schaep, D. Wilms, C. Vandecasteele, Influence of molecular size, polarity and charge on the retention of organic molecules by nanofiltration, *J. Membr. Sci.*, 156 (1999) 29–41.
- [44] B. González, N. Calvar, E. Gómez, Á. Domínguez, Density, dynamic viscosity, and derived properties of binary mixtures of methanol or ethanol with water, ethyl acetate, and methyl acetate at $T = (293.15, 298.15, \text{ and } 303.15) \text{ K}$, *J. Chem. Thermodyn.*, 39 (2007) 1578–1588.
- [45] F.-M. Pang, C.-E. Seng, T.-T. Teng, M.H. Ibrahim, Densities and viscosities of aqueous solutions of 1-propanol and 2-propanol at temperatures from 293.15 K to 333.15 K, *J. Mol. Liq.*, 136 (2007) 71–78.
- [46] I.S. Khattab, F. Bandarkar, M.A.A. Fakhree, A. Jouyban, Density, viscosity, and surface tension of water-ethanol mixtures from 293 to 323 K, *Korean J. Chem. Eng.*, 29 (2012) 812–817.
- [47] <https://wissen.science-and-fun.de/chemistry/chemistry/density-tables/ethanol-water-mixtures/>
- [48] T.V.N. Nguyen, Etudes des mécanismes de transfert des solutés neutres et chargés en nanofiltration dans des milieux hydroalcooliques (Studies of transfer mechanisms of neutral and charged solutes in nanofiltration in hydroalcoholic media), Ph.D. Dissertation, Université de Rennes 1, France, 2018.